

5 February 2020, Product Demo at Photonics West 2020

Diffractive and Metasurfaces: from Function to Structure Simulation Seamlessly in VirtualLab Fusion

Stefan Steiner, PhD

LightTrans International UG

Jena, Germany

Teams



LightTrans (since 1999)

- Optical technologies development
- Technical support, seminars, and trainings
- Engineering projects
- Distribution of VirtualLab Fusion, together with distributors worldwide



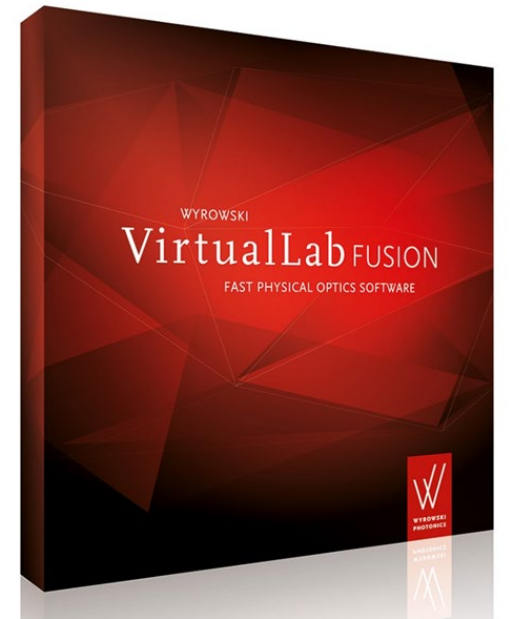
(since 2014)



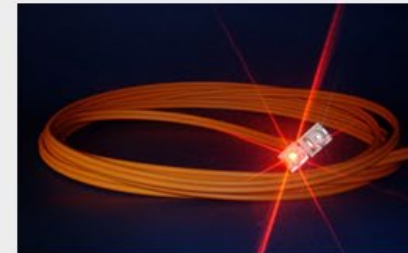
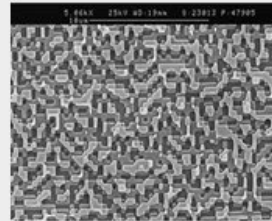
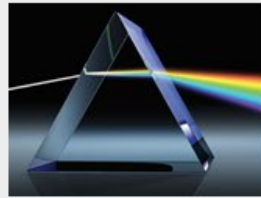
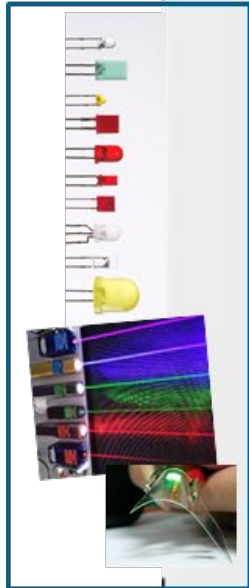
photo from wikitravel

Optical Design Software and Services

**Booth #4545
(German pavilion)**



Physical-Optics System Modeling

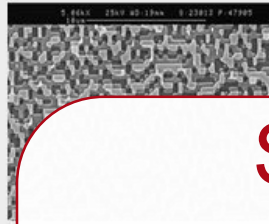
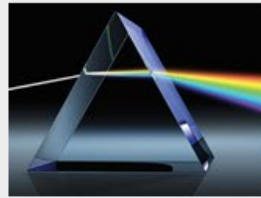
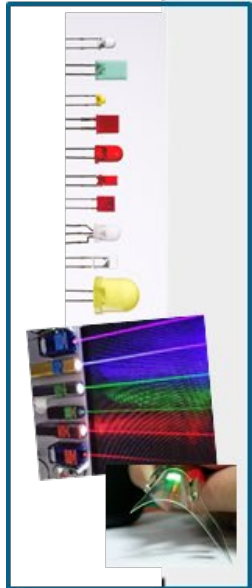


Name	Integral equations	Differential equations
Gauss's law	$\oiint_{\partial\Omega} \mathbf{E} \cdot d\mathbf{S} = \frac{1}{\epsilon_0} \iiint_{\Omega} \rho dV$	$\nabla \cdot \mathbf{E} = \frac{\rho}{\epsilon_0}$
Gauss's law for magnetism	$\oiint_{\partial\Omega} \mathbf{B} \cdot d\mathbf{S} = 0$	$\nabla \cdot \mathbf{B} = 0$
Maxwell-Faraday equation (Faraday's law of induction)	$\oint_{\partial\Sigma} \mathbf{E} \cdot d\boldsymbol{\ell} = -\frac{d}{dt} \iint_{\Sigma} \mathbf{B} \cdot d\mathbf{S}$	$\nabla \times \mathbf{E} = -\frac{\partial \mathbf{B}}{\partial t}$
Ampère's circuital law (with Maxwell's addition)	$\oint_{\partial\Sigma} \mathbf{B} \cdot d\boldsymbol{\ell} = \mu_0 \iint_{\Sigma} \mathbf{J} \cdot d\mathbf{S} + \mu_0 \epsilon_0 \frac{d}{dt} \iint_{\Sigma} \mathbf{E} \cdot d\mathbf{S}$	$\nabla \times \mathbf{B} = \mu_0 \left(\mathbf{J} + \epsilon_0 \frac{\partial \mathbf{E}}{\partial t} \right)$

Homogeneous

Solve Maxwell's equations for given source field and components.

Physical-Optics System Modeling

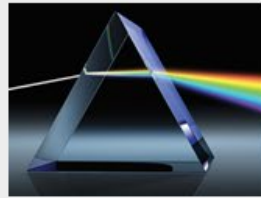
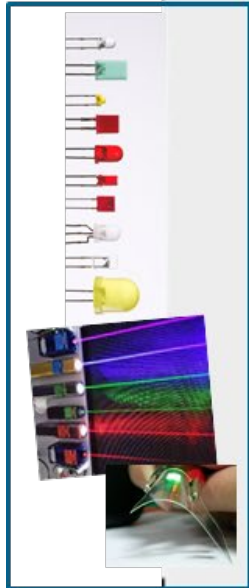


Name	Integral equations	Differ
Gauss's law	$\oiint_{\partial\Omega} \mathbf{E} \cdot d\mathbf{S} = \frac{1}{\epsilon_0} \iiint_{\Omega} \rho dV$	$\nabla \cdot \mathbf{E} = \frac{\rho}{\epsilon_0}$
Gauss's law for magnetism	$\oiint_{\partial\Omega} \mathbf{B} \cdot d\mathbf{S} = 0$	$\nabla \cdot \mathbf{B} = 0$
Maxwell-Faraday equation (Faraday's law of induction)	$\oint_{\partial\Sigma} \mathbf{E} \cdot d\boldsymbol{\ell} = -\frac{d}{dt} \iint_{\Sigma} \mathbf{B} \cdot d\mathbf{S}$	$\nabla \times \mathbf{E} = -\frac{d\mathbf{B}}{dt}$
Ampère's circuital law (with Maxwell's addition)	$\oint_{\partial\Sigma} \mathbf{B} \cdot d\boldsymbol{\ell} = \mu_0 \iint_{\Sigma} \mathbf{J} \cdot d\mathbf{S} + \mu_0 \epsilon_0 \frac{d}{dt} \iint_{\Sigma} \mathbf{E} \cdot d\mathbf{S}$	$\nabla \times \mathbf{B} = \mu_0 (\mathbf{J} + \epsilon_0 \frac{d\mathbf{E}}{dt})$

Homogen

Solution of Maxwell's equations with one field solver, e.g. FEM, FMM, or FDTD, for entire system not feasible because of numerical effort!

Physical-Optics System Modeling

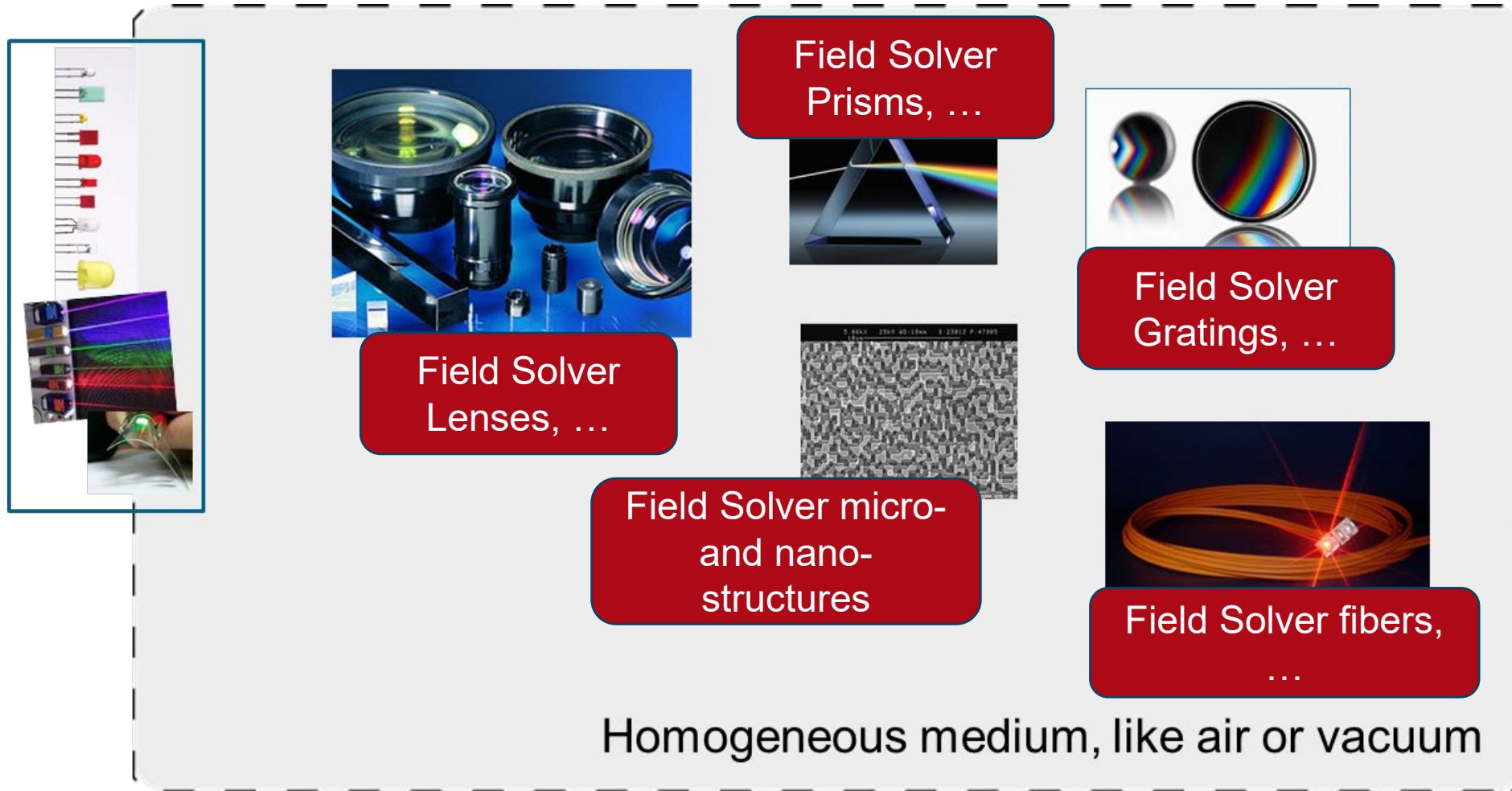


Name	Integral equations
Gauss's law	$\oiint_{\partial\Omega} \mathbf{E} \cdot d\mathbf{S} = \frac{1}{\epsilon_0} \iiint_{\Omega} \rho dV$
Gauss's law for magnetism	$\oiint_{\partial\Omega} \mathbf{B} \cdot d\mathbf{S} = 0$
Maxwell-Faraday equation (Faraday's law of induction)	$\oint_{\partial\Sigma} \mathbf{E} \cdot d\boldsymbol{\ell} = -\frac{d}{dt} \iint_{\Sigma} \mathbf{B} \cdot d\mathbf{S}$
Ampère's circuital law (with Maxwell's addition)	$\oint_{\partial\Sigma} \mathbf{B} \cdot d\boldsymbol{\ell} = \mu_0 \iint_{\Sigma} \mathbf{J} \cdot d\mathbf{S} + \mu_0 \epsilon_0 \frac{d}{dt} \iint_{\Sigma} \mathbf{E} \cdot d\mathbf{S}$

Homogeneous medium, like air or vacuum

How to obtain a reliable and fast physical optics solution - whenever possible?

Connecting Optical Technologies / Maxwell Solvers



Connecting Optical Technologies / Maxwell Solvers

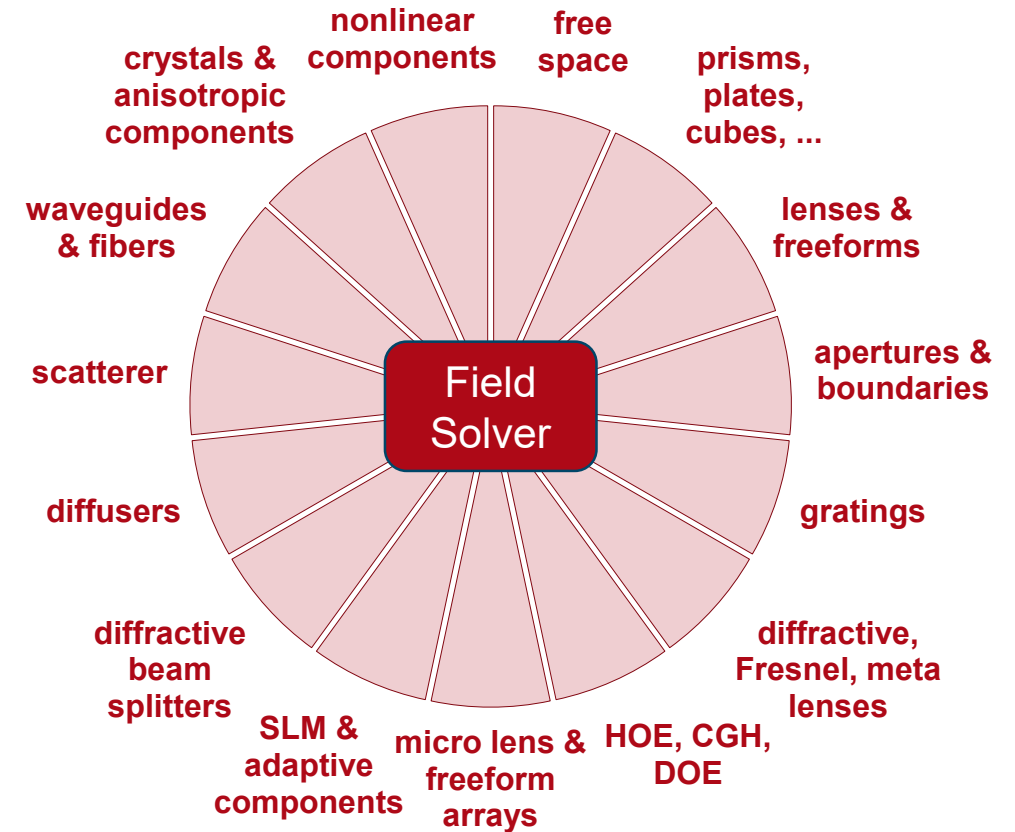
Problem:

Application of a single field solver, e.g. FEM or FDTD, to the entire system:

Unrealistic numerical effort

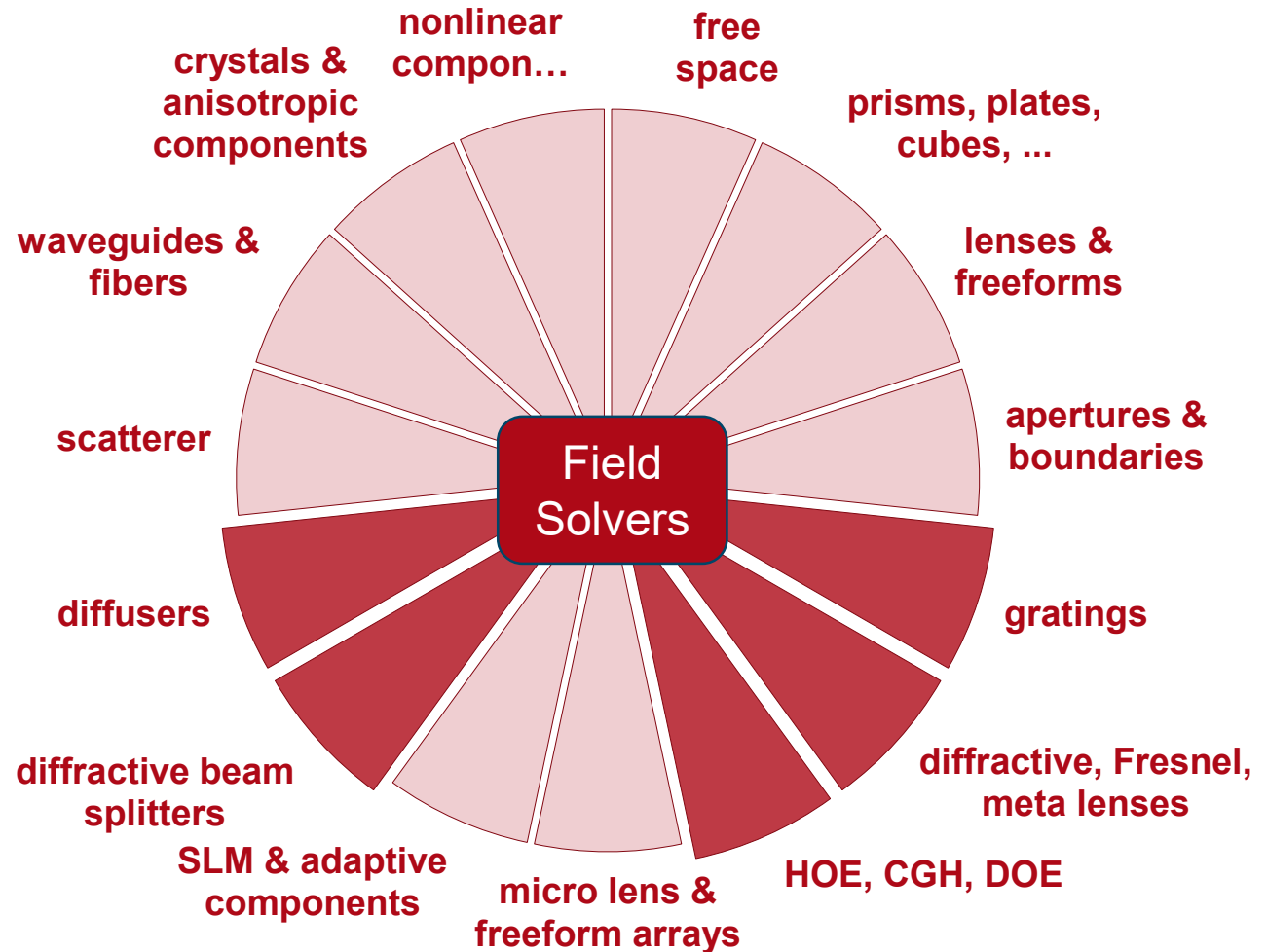
Solution:

- Decomposition of system and application of regional field solvers.
- Interconnection of different solvers and so to solve the complete system.

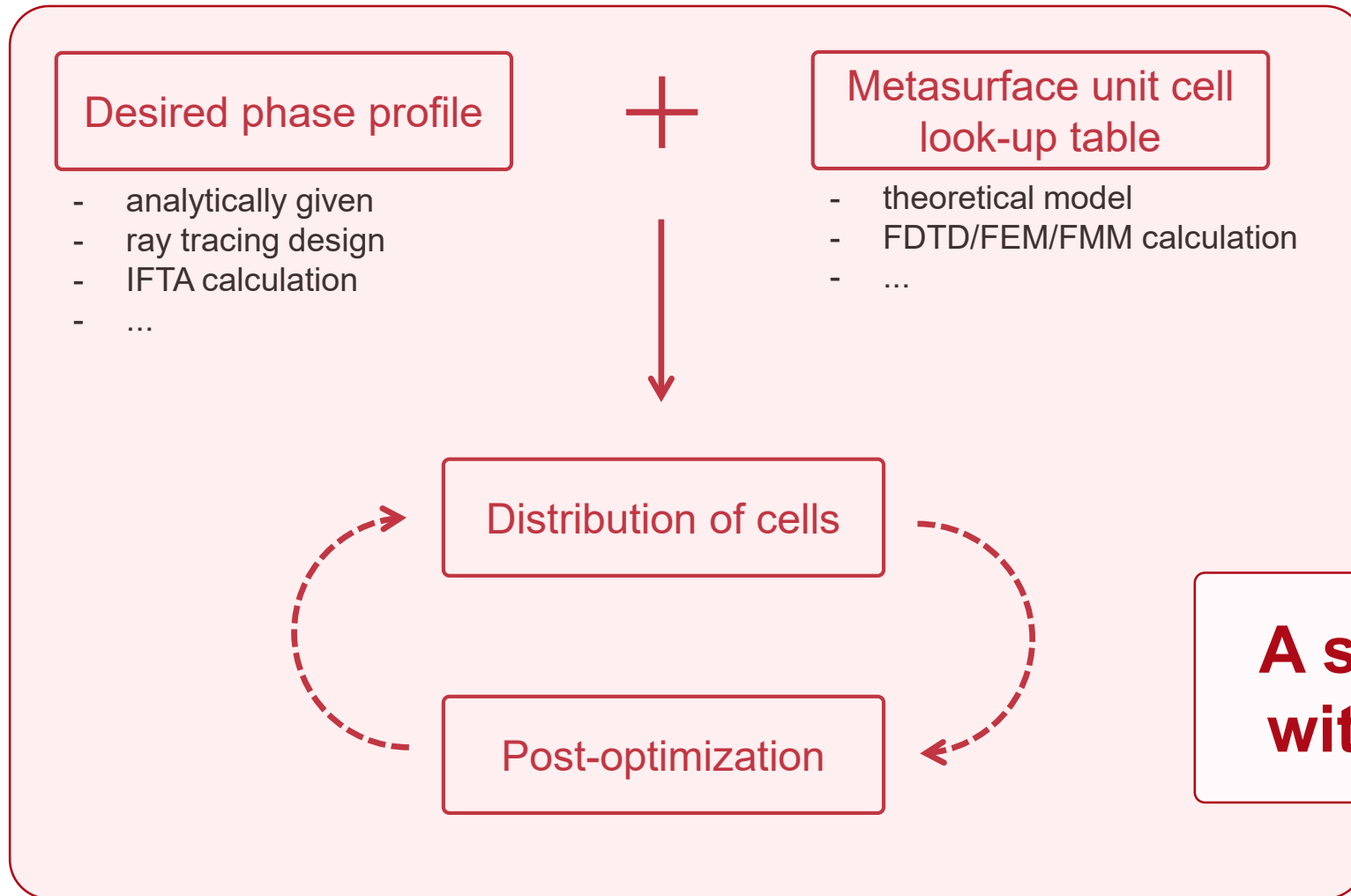


VirtualLab Fusion – Diffractive Optics Applications

Selection of
VirtualLab Fusion
applications for
metasurfaces



General Design Procedure



State-of-the-art: exchange between several different software programmes, e.g., ray tracer, FDTD solver, and Matlab ...

A seamless workflow within one platform?

Blazed Meta-Grating Composed of Square Pillars

 P. Lalanne, *et al.*, "Blazed binary subwavelength gratings with efficiencies larger than those of conventional échelette gratings," *Opt. Lett.* 23, 1081-1083 (1998)

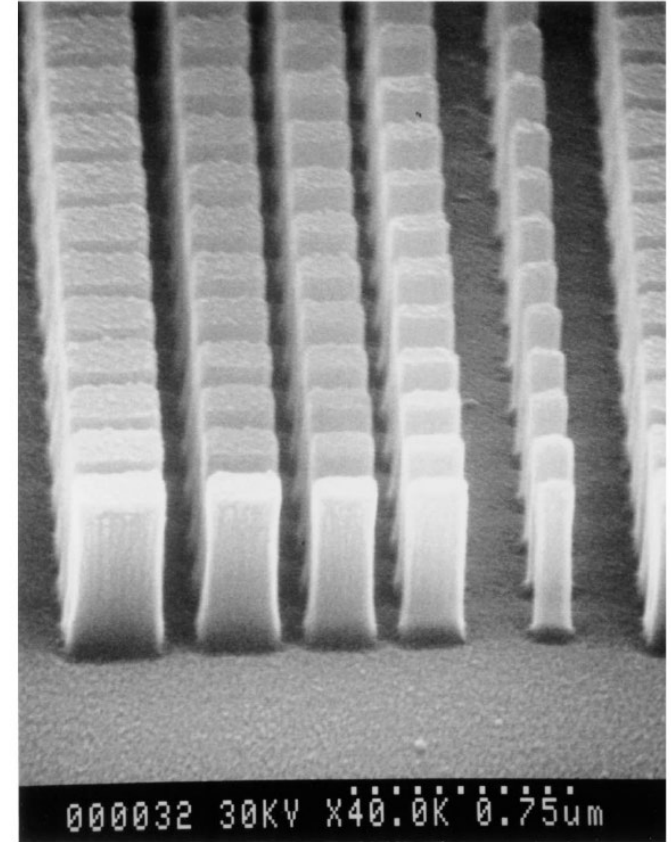
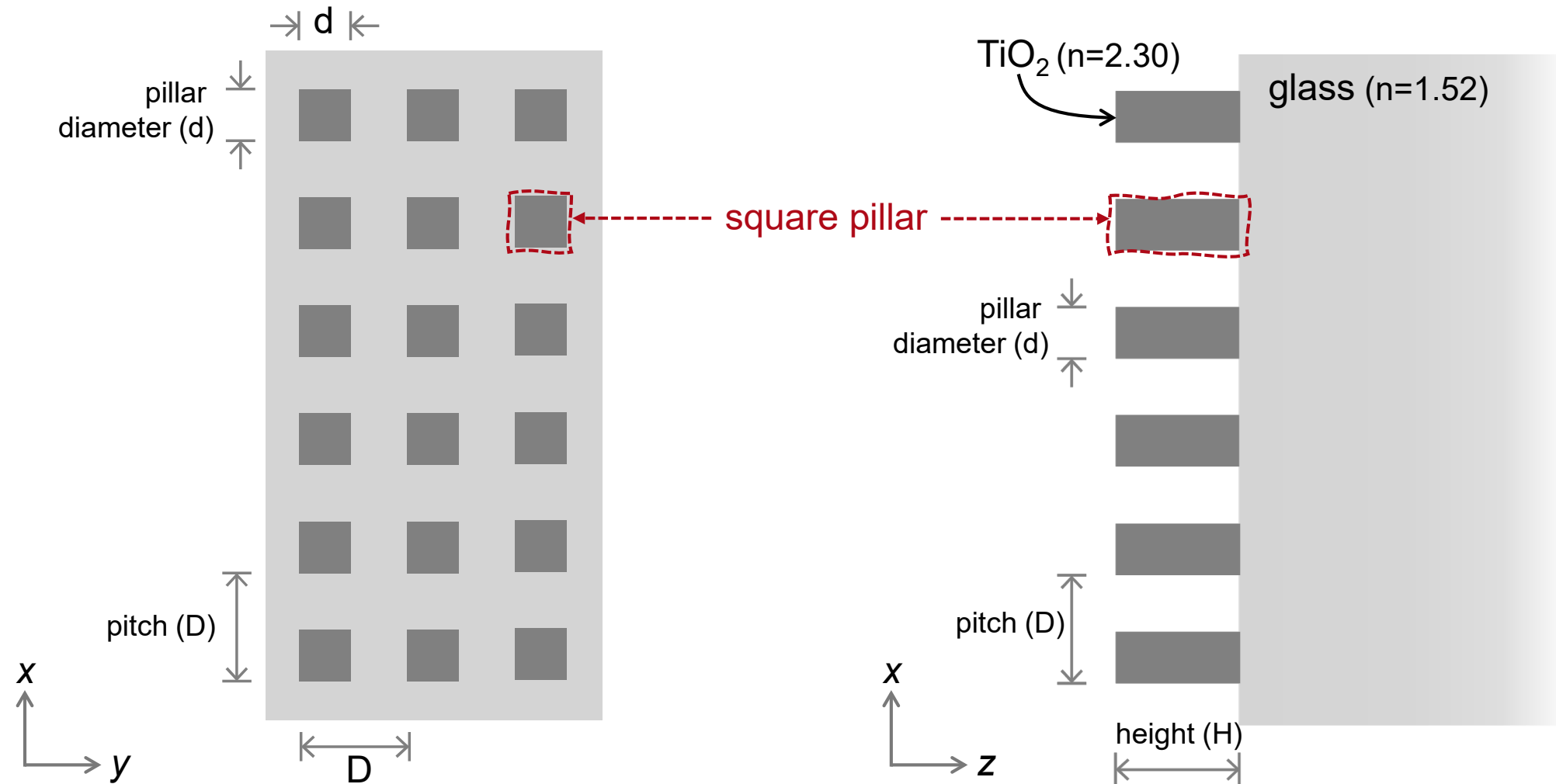
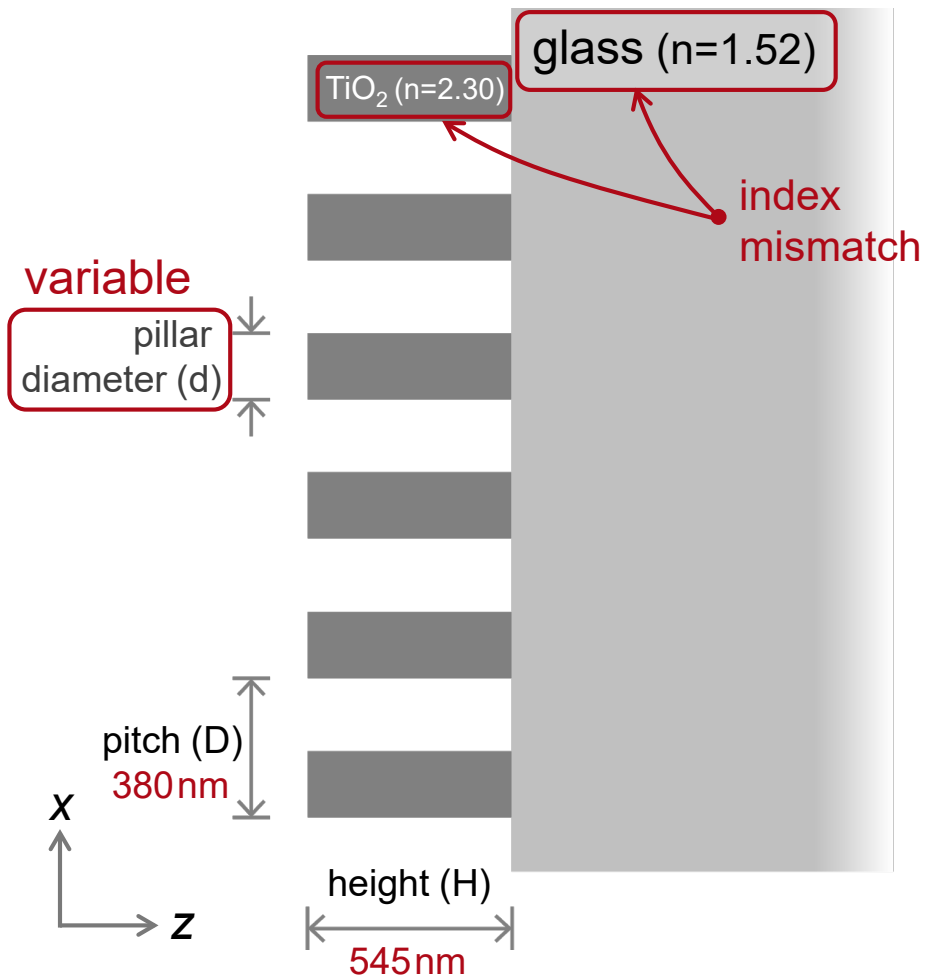


Fig. 2. Scanning-electron micrograph of the blazed binary subwavelength grating. The horizontal period (along the x axis) is $1.9 \mu\text{m}$, and the period in the perpendicular direction (y axis) is equal to the sampling period (380 nm). The maximum pillar aspect ratio is 4.6.

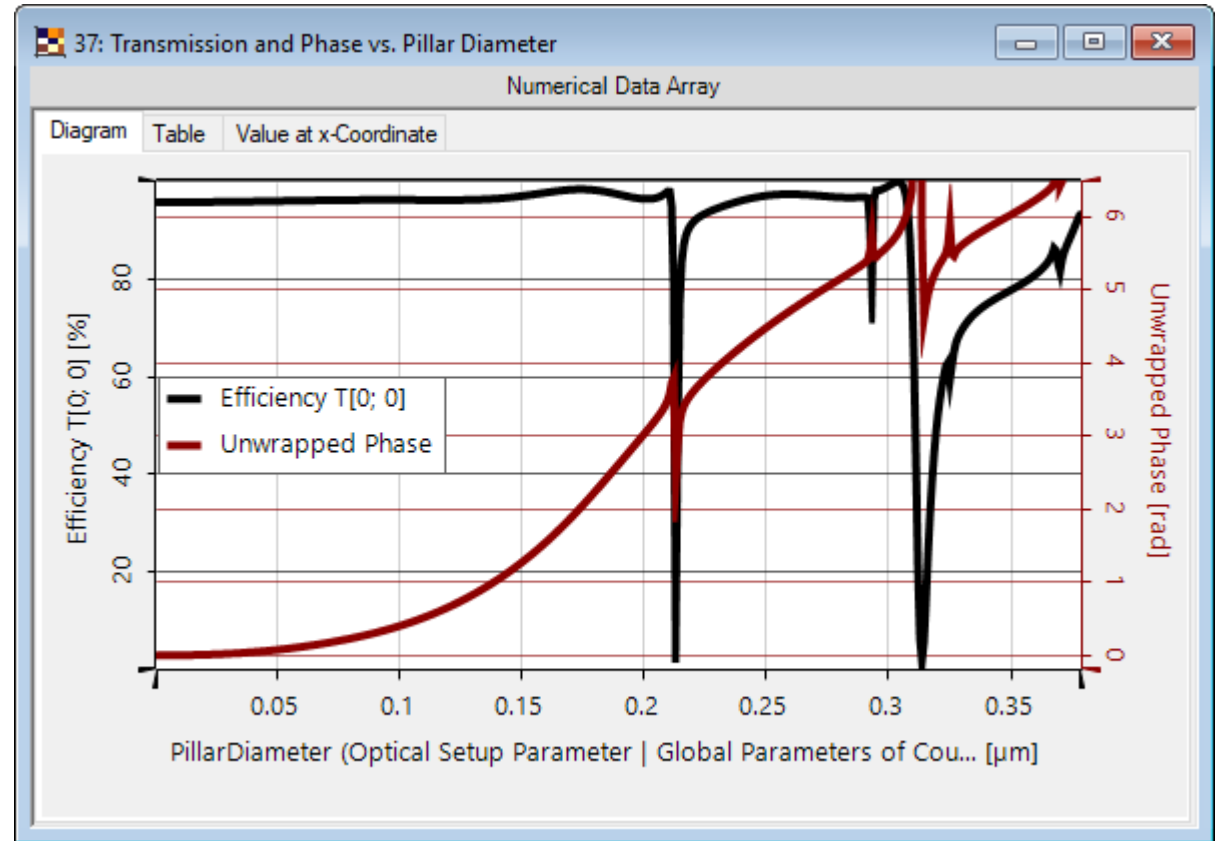
Building Block / Unit Cell Analysis



Building Block / Unit Cell Analysis

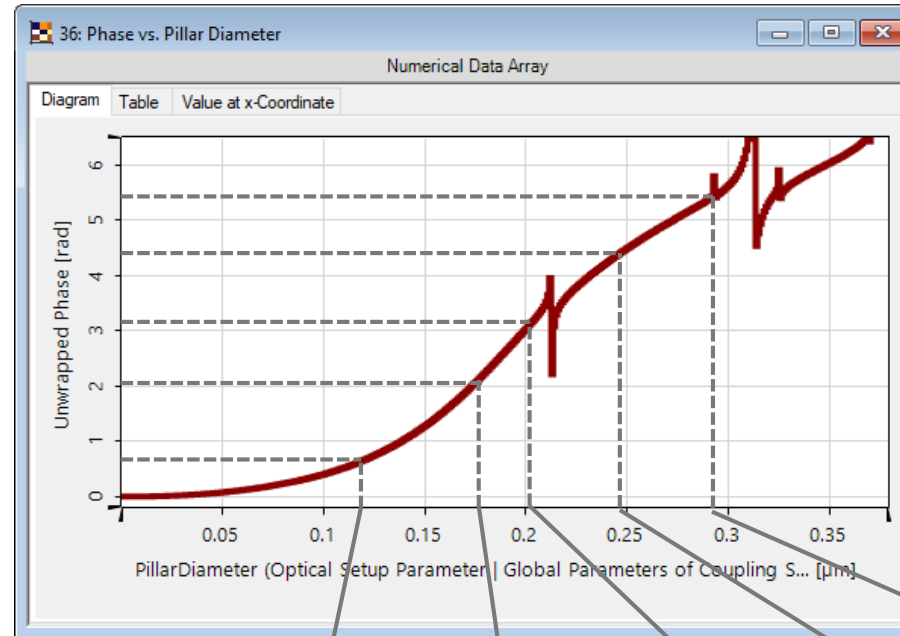
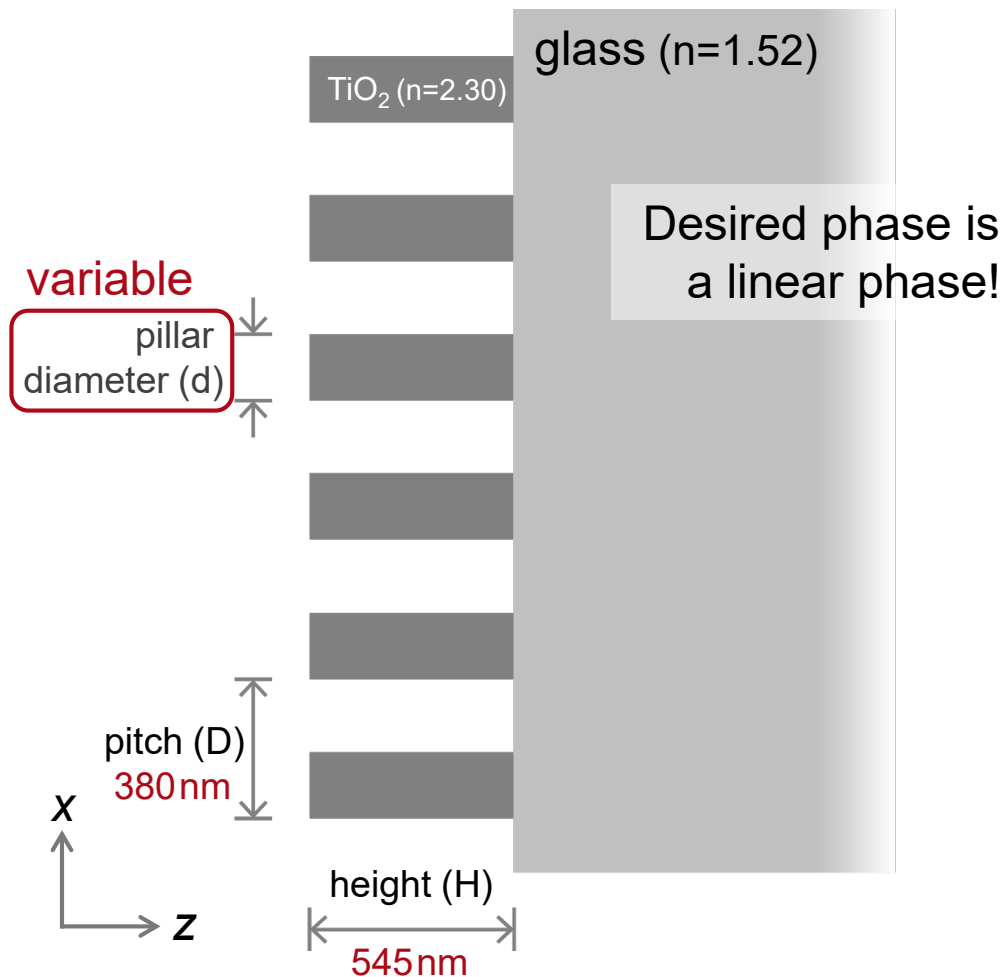


transmission amplitude/phase vs. pillar diameter (@633nm)



Blazed Metagrating_01_Single Pillar ...

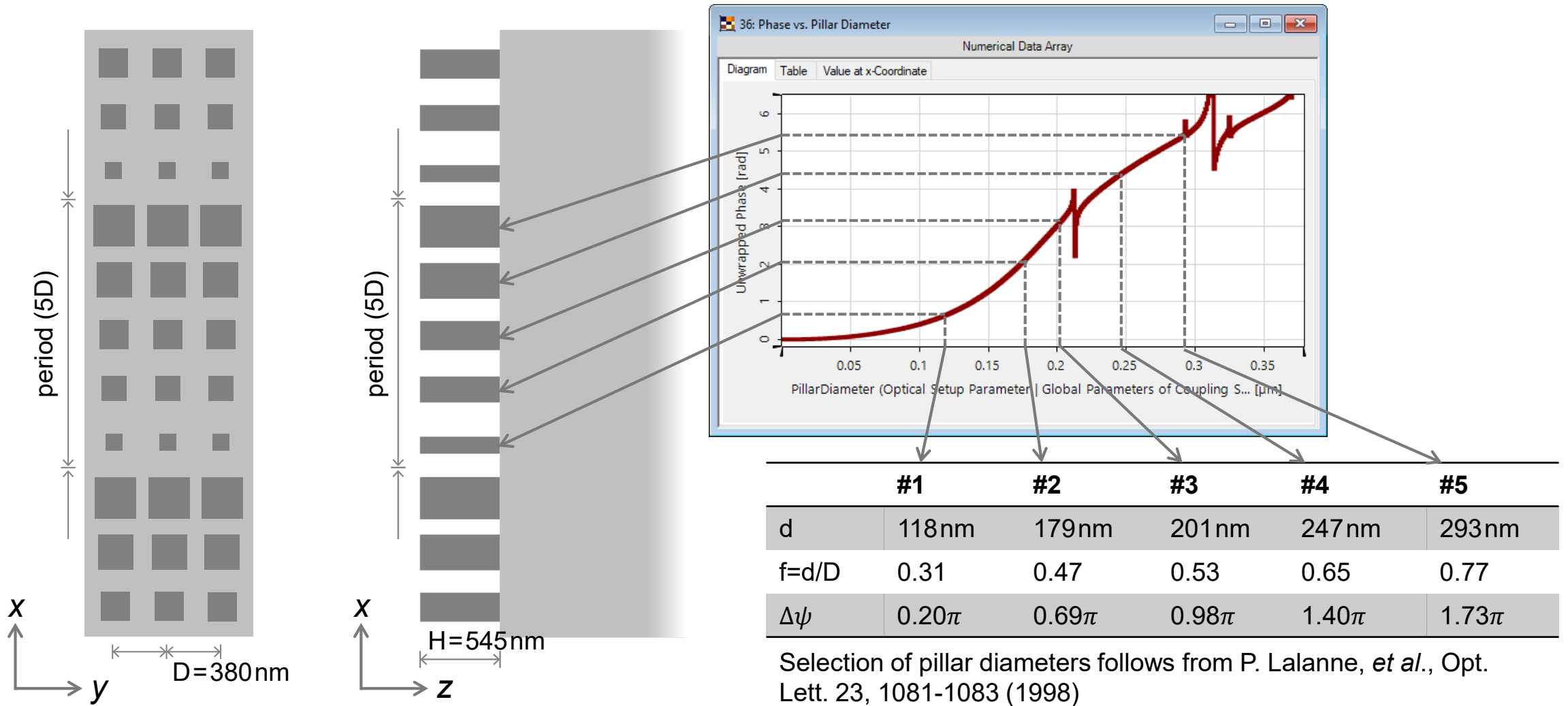
Distribution of Cells → Linear Phase



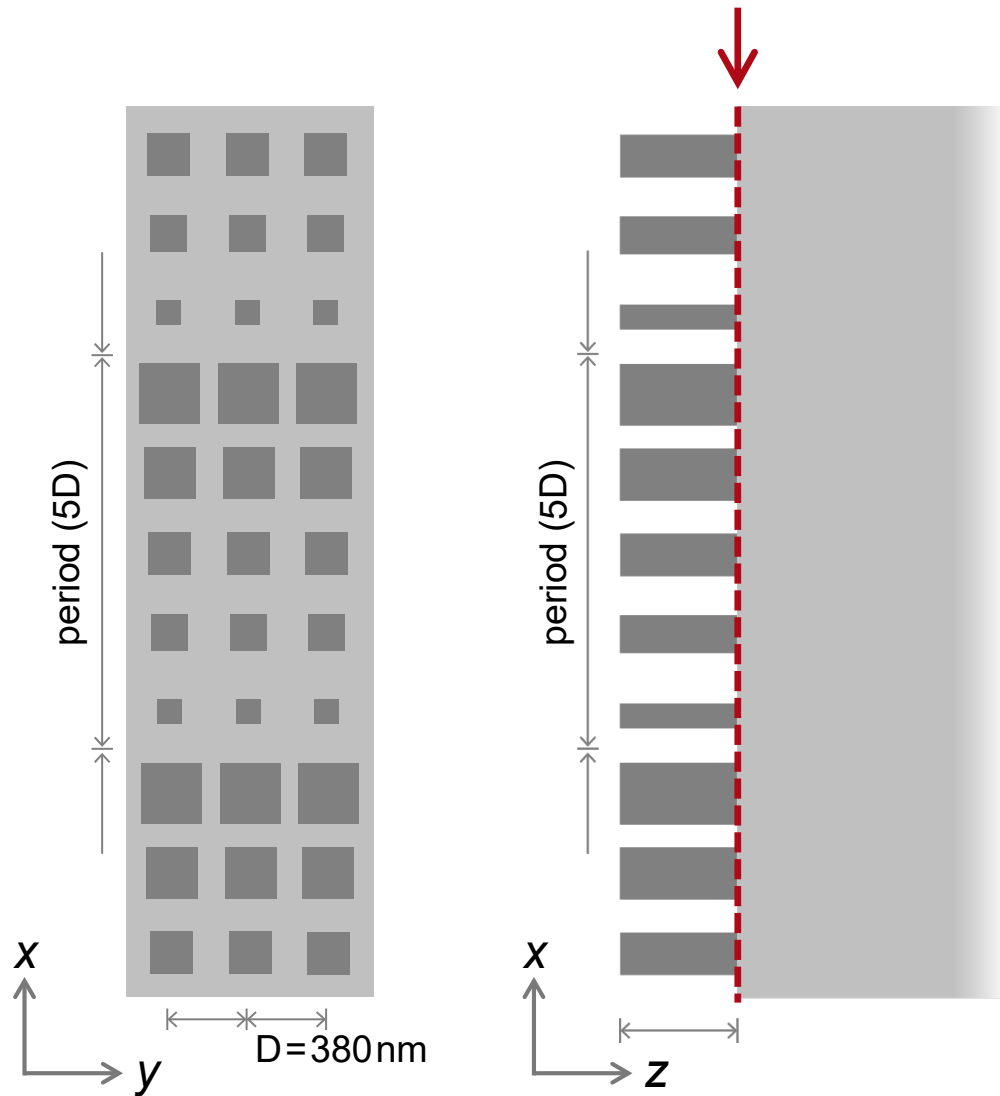
	#1	#2	#3	#4	#5
d	118 nm	179 nm	201 nm	247 nm	293 nm
f=d/D	0.31	0.47	0.53	0.65	0.77
$\Delta\psi$	0.20π	0.69π	0.98π	1.40π	1.73π

Selection of pillar diameters follows from P. Lalanne, *et al.*, Opt. Lett. 23, 1081-1083 (1998)

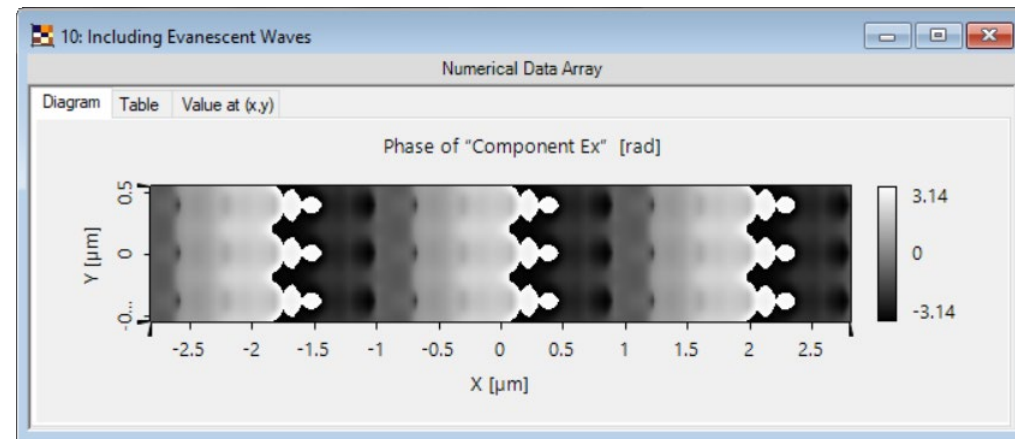
Distribution of Cells → Linear Phase



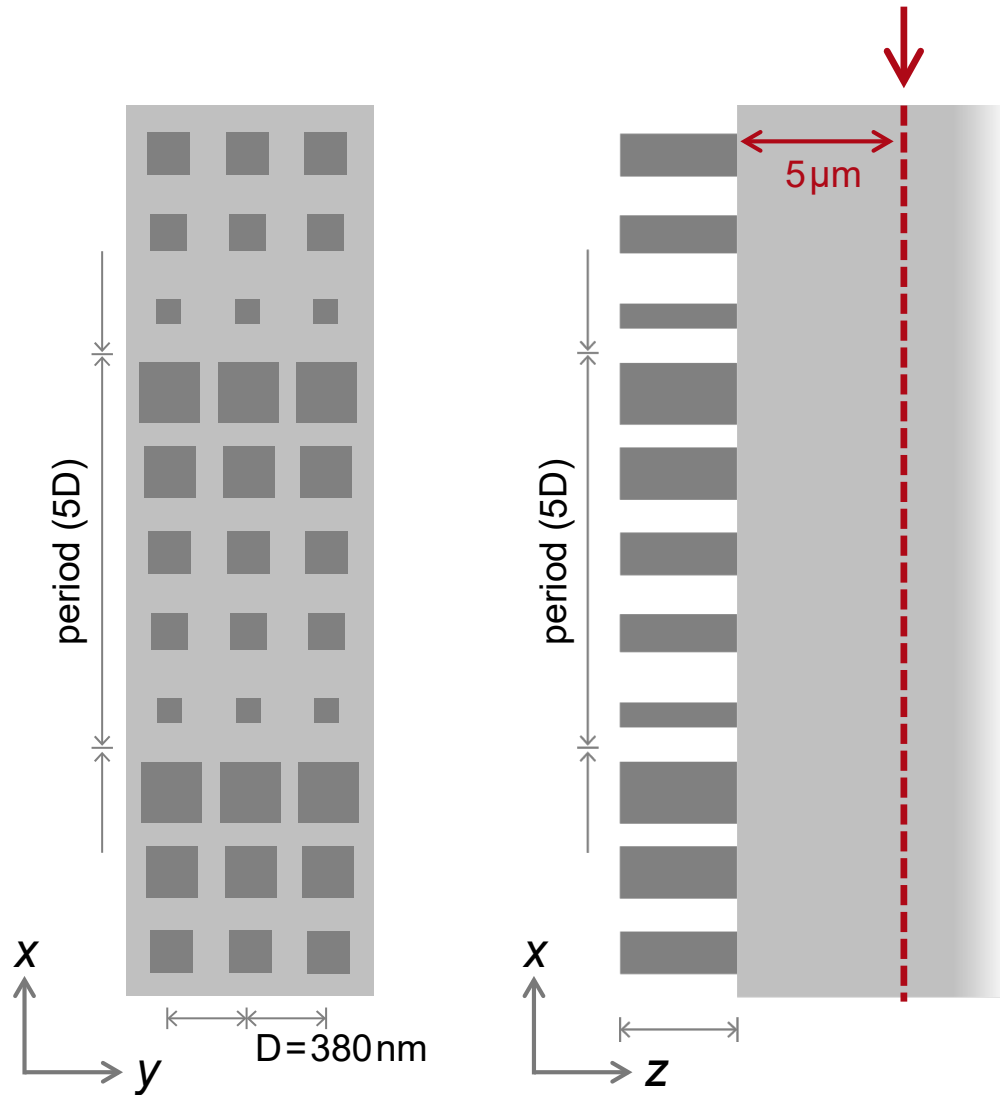
Performance Evaluation: Transmitted Phase Distribution



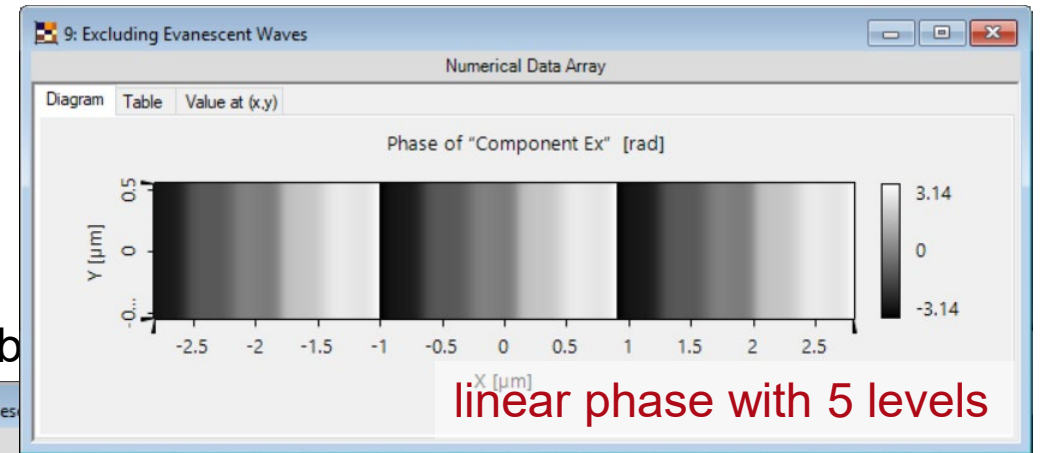
directly behind the grating



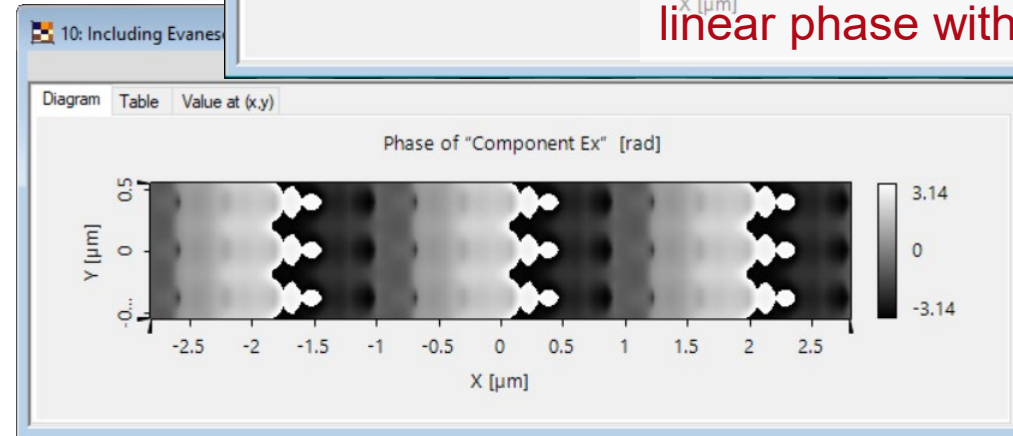
Performance Evaluation: Transmitted Phase Distribution



5 μm behind the grating (evanescent waves damped)

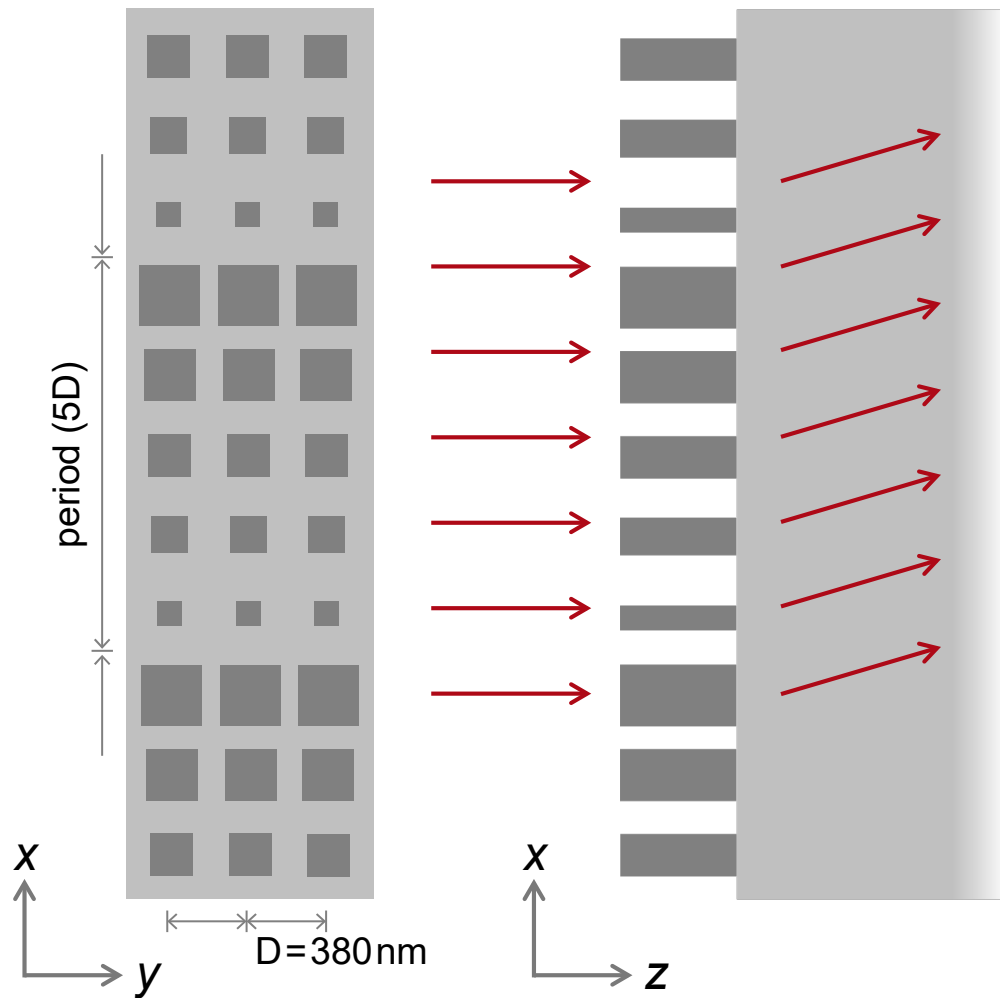


directly b



Blazed Metagrating_02_Initial Blazed Grating

Performance Evaluation: Diffraction Efficiency



grating performance evaluation

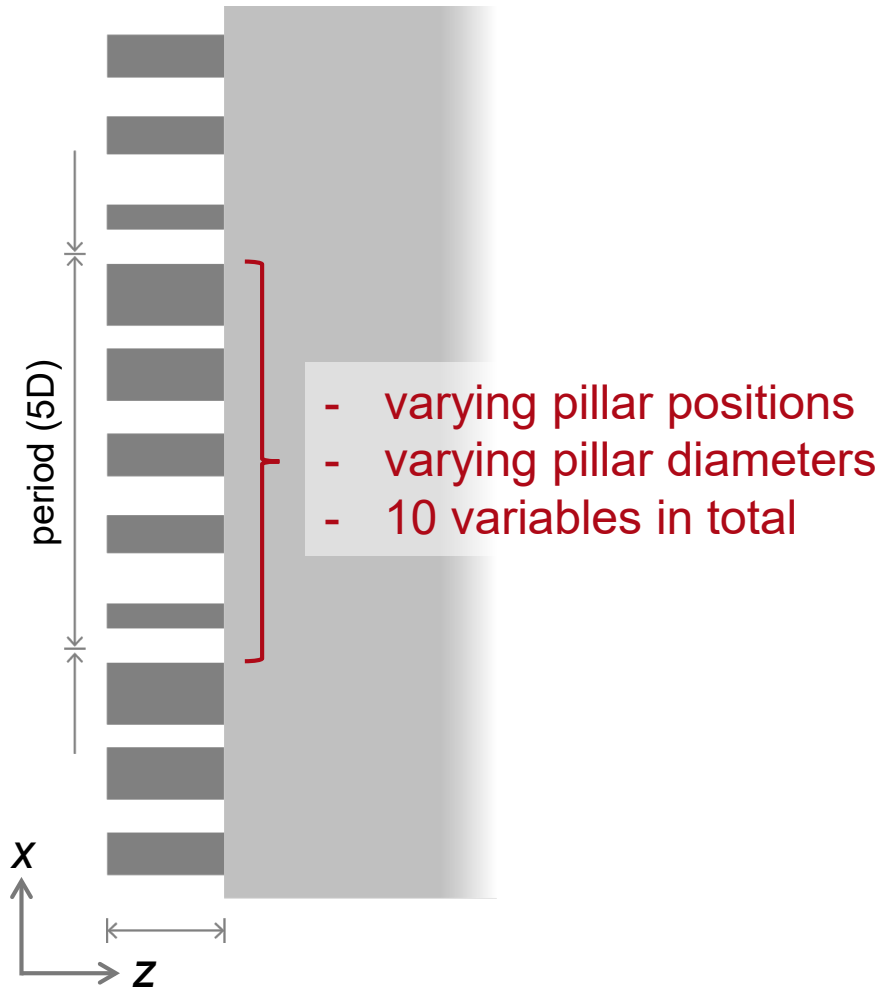
	Efficiency
TE-polarization	80.2%
TM-polarization	74.2%
Average	77.2%

Same average efficiency value reported in
P. Lalanne, *et al.*, Opt. Lett. 23, 1081-1083 (1998)

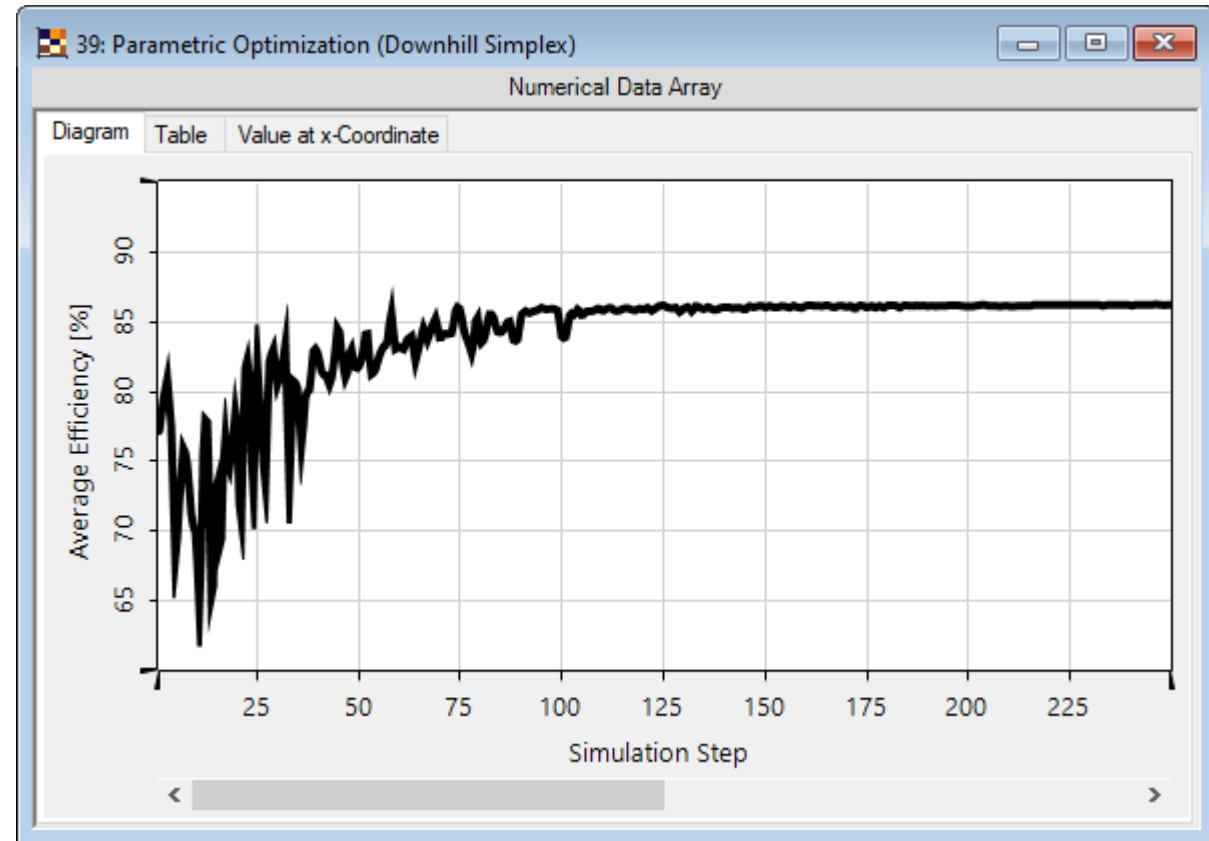


Blazed Metagrating_02_Initial Blazed Grating

Post-Optimization of Metagrating

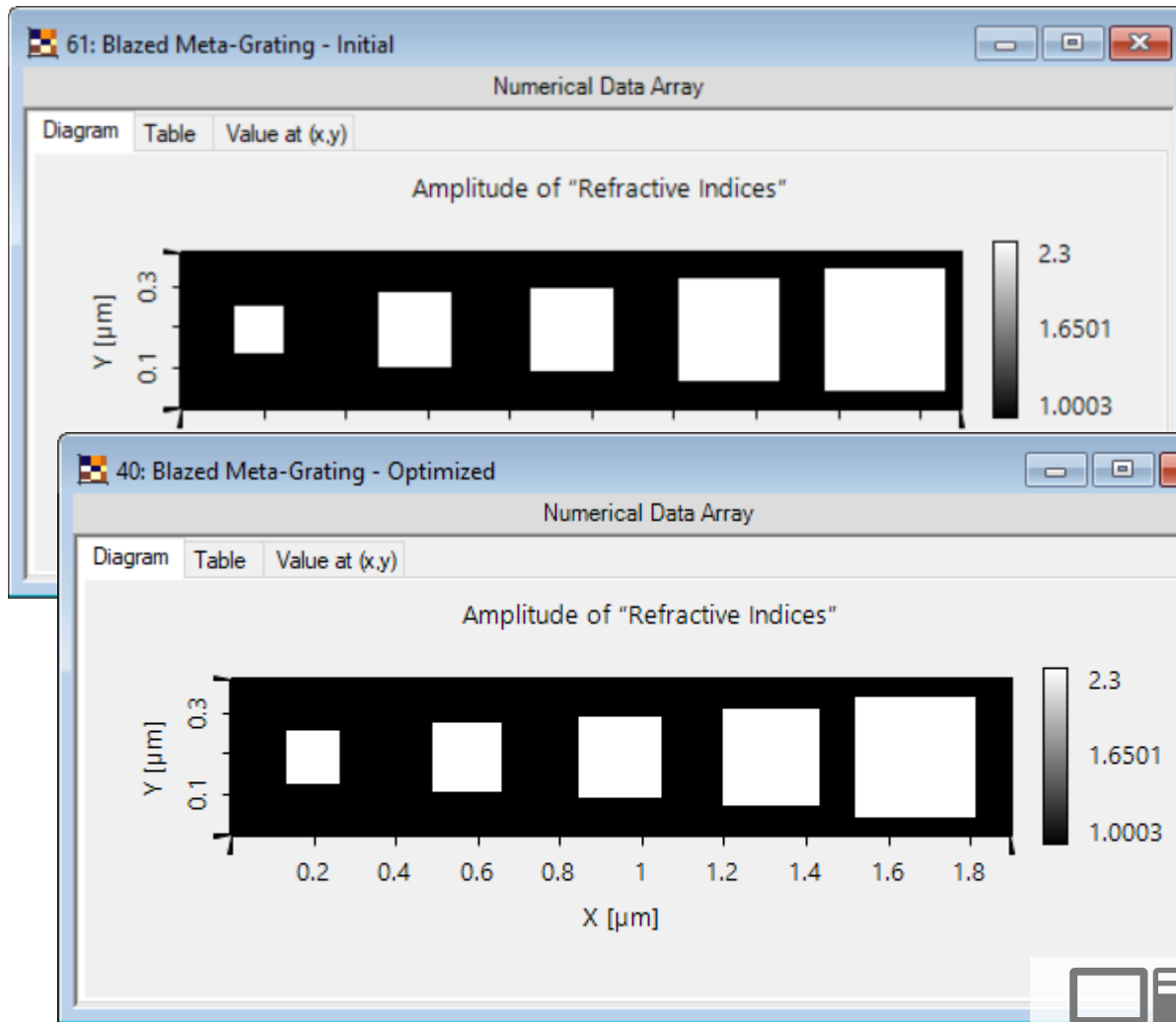


downhill simplex optimization with FMM/RCWA for grating analysis



Blazed Metagrating_03_Parametric Optimization

Post-Optimization: Initial vs. Optimized Structure



	Efficiency
TE-polarization	80.2%
TM-polarization	74.2%
Average	77.2%

	Efficiency
TE-polarization	85.5%
TM-polarization	87.0%
Average	86.3%

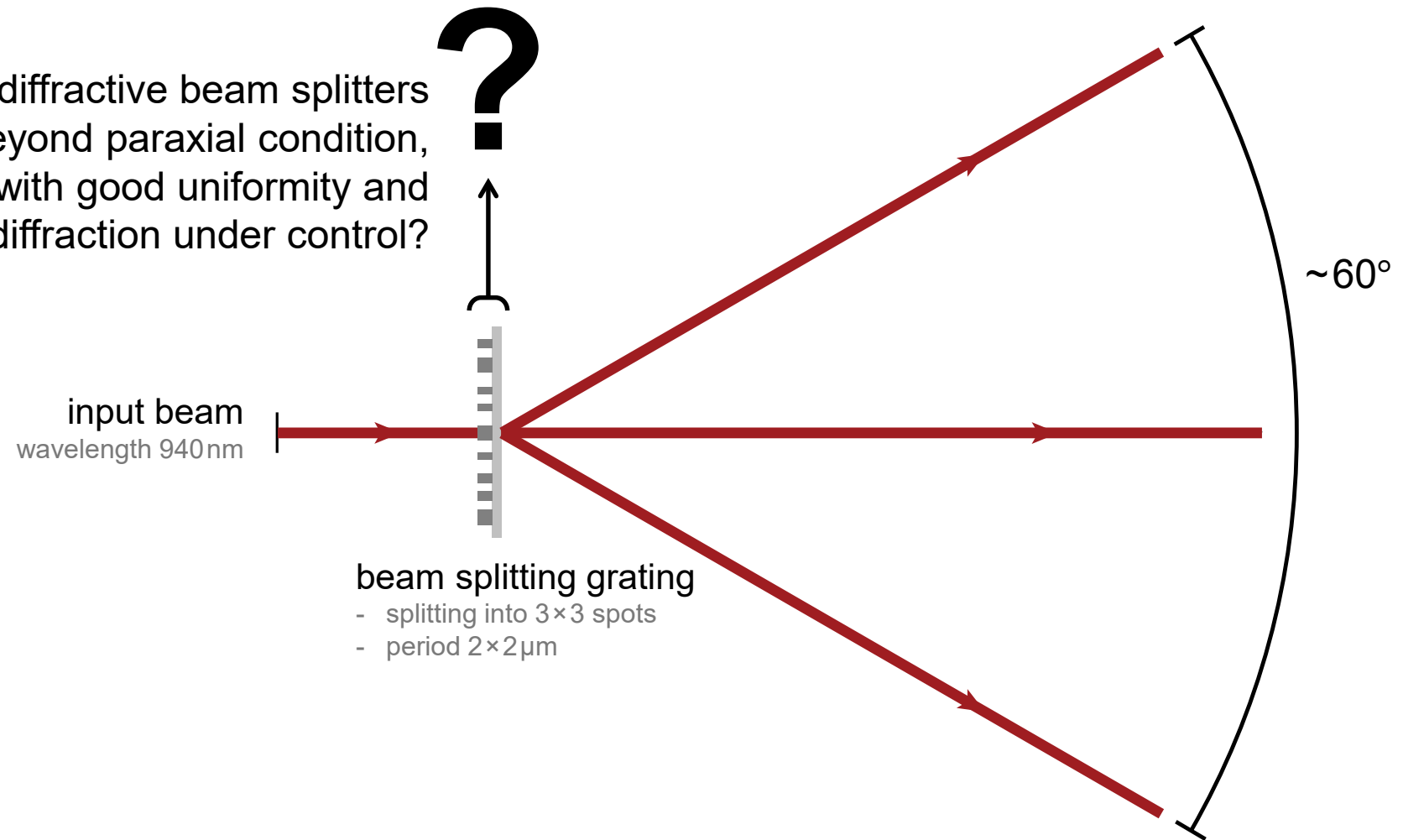


Blazed Metagrating_04_Optimized Blazed Grating

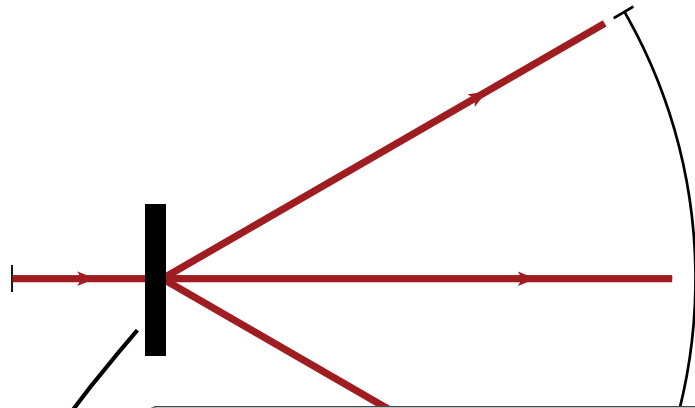
Design of Meta-Grating as Large-Angle Spot Projector

Design Task

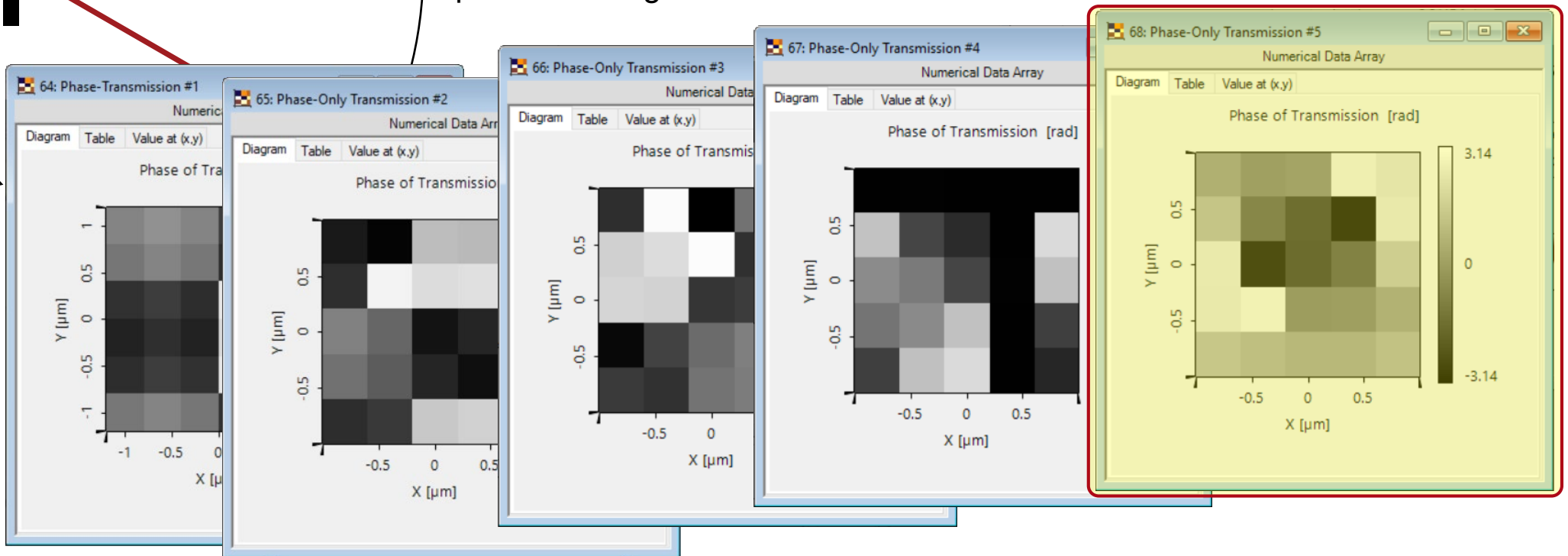
How to design diffractive beam splitters that work beyond paraxial condition, especially with good uniformity and zeroth-order diffraction under control?



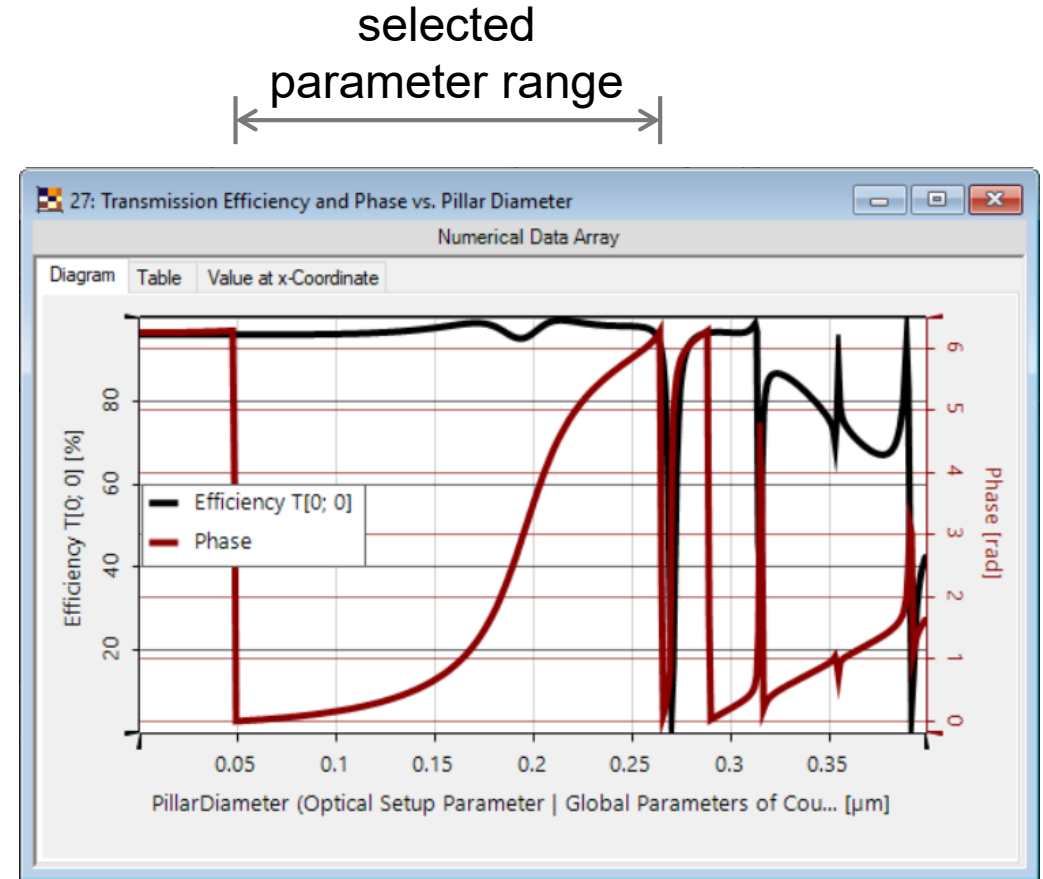
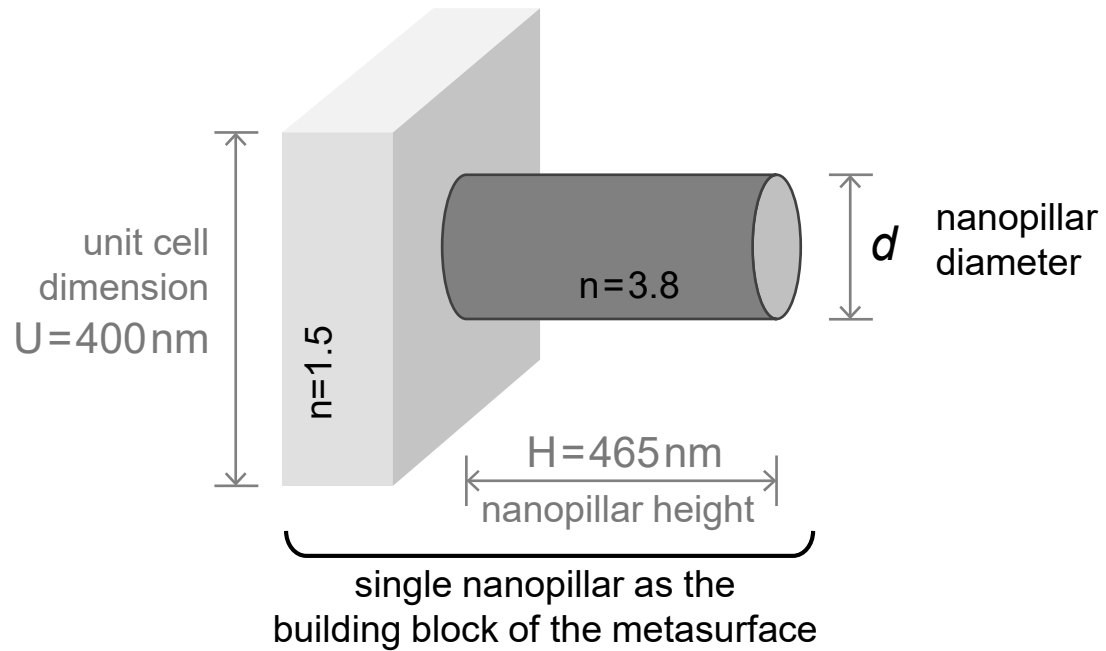
Desired Phase Profile Design (IFTA)



With differently random phase distributions as starting points, IFTA calculates different possible design results.



Building Block / Unit Cell Analysis



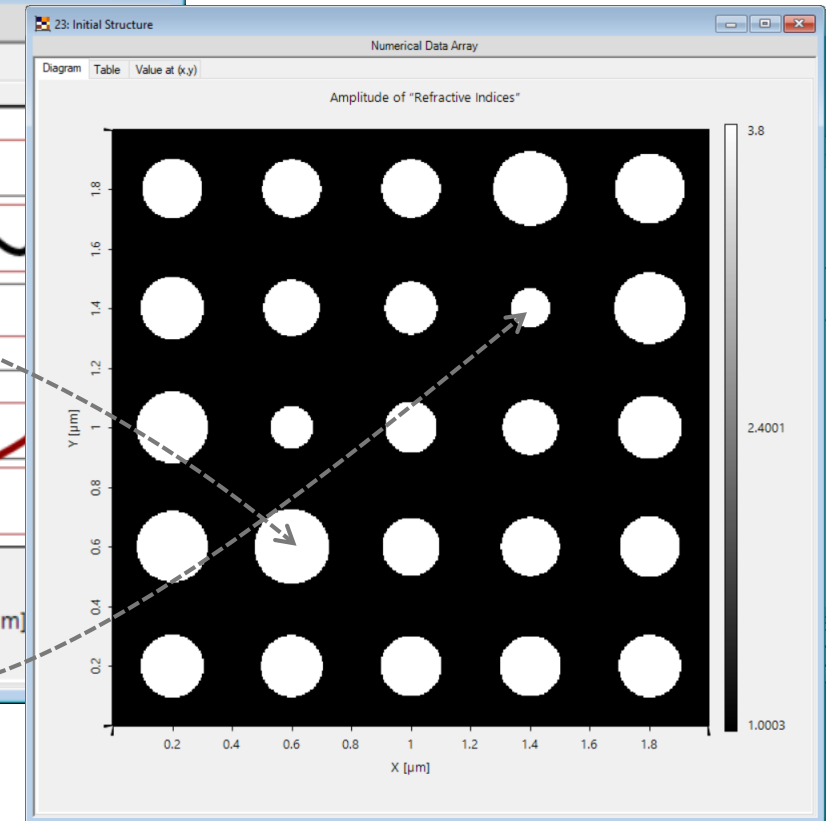
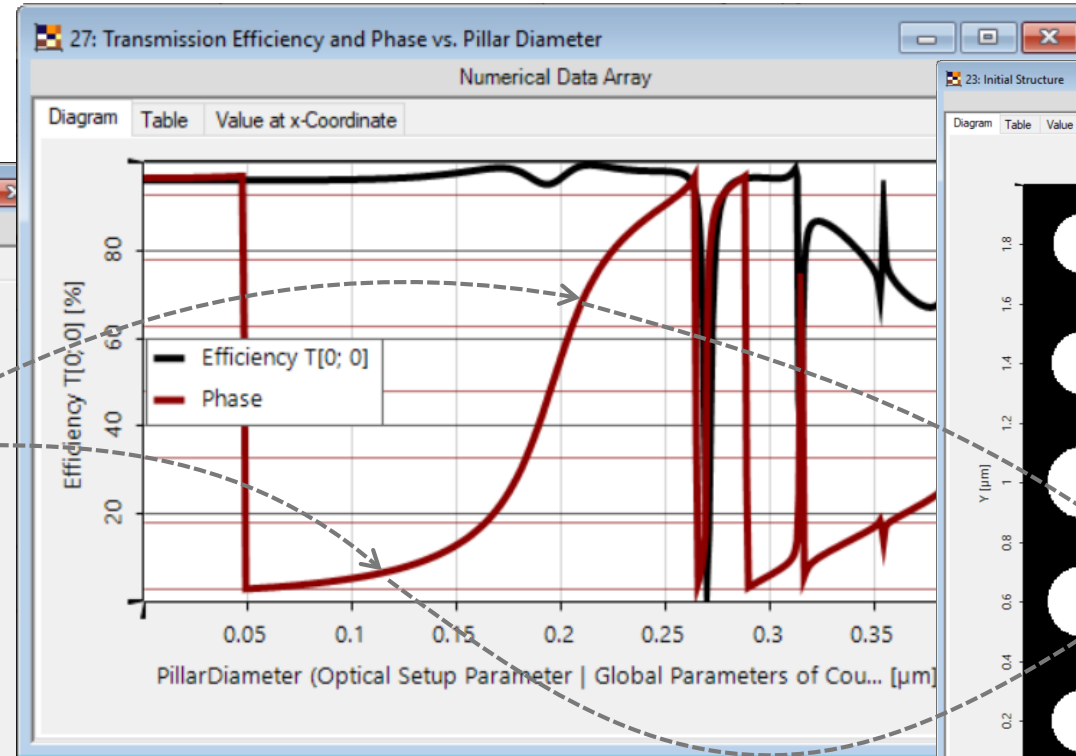
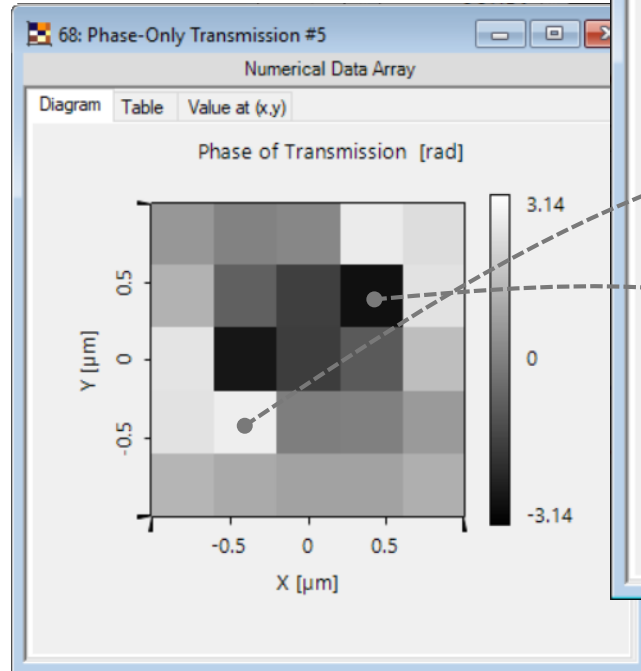
2D Metagrating_01_Single Pillar Analysis ...

Distribution of Cells

phase-diameter map / library

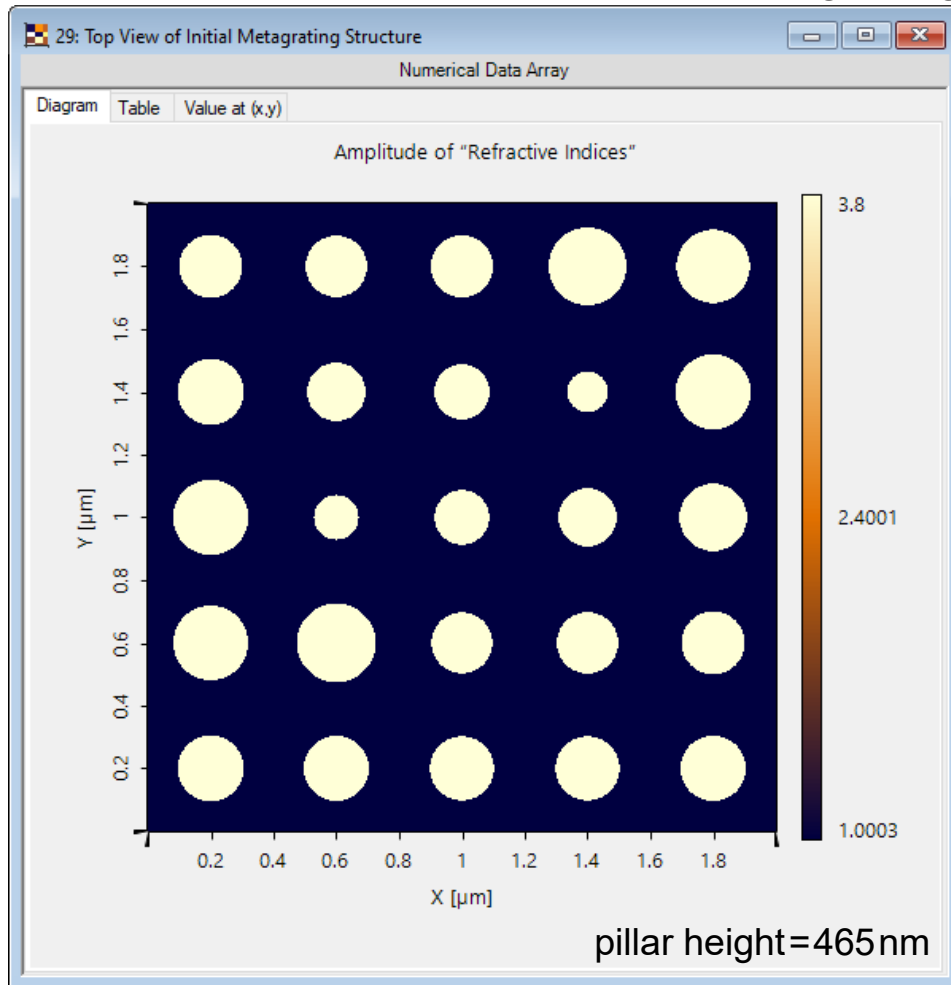
metasurface structure

phase-only transmission

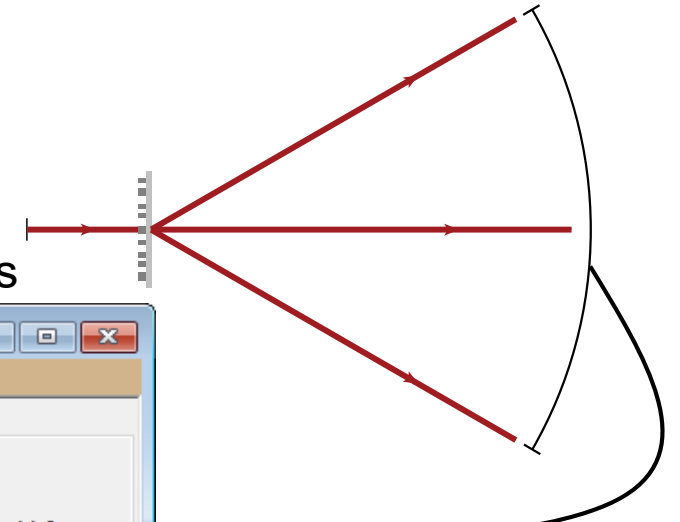
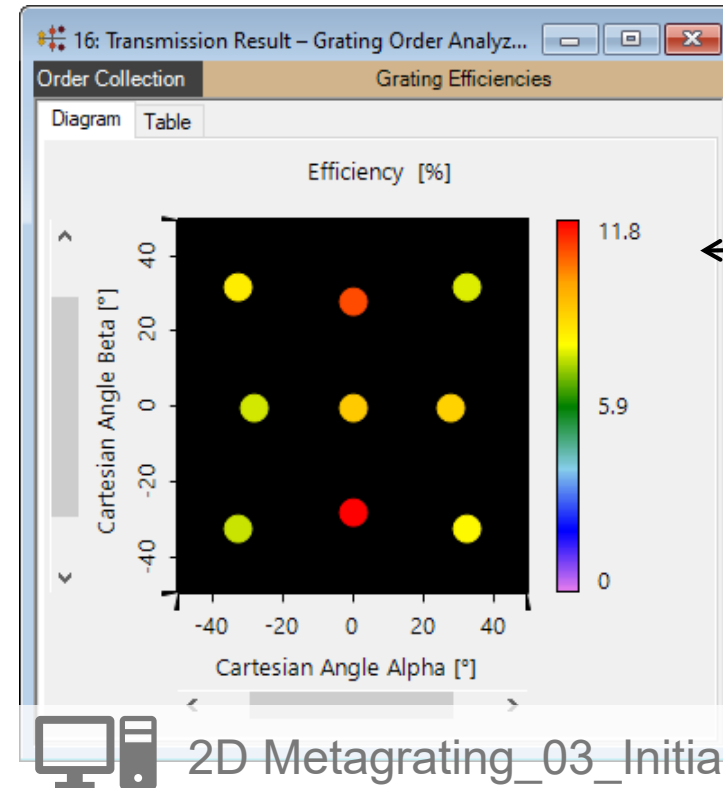


Performance Evaluation: Initial Design

top view of initial metagrating



diffraction efficiencies

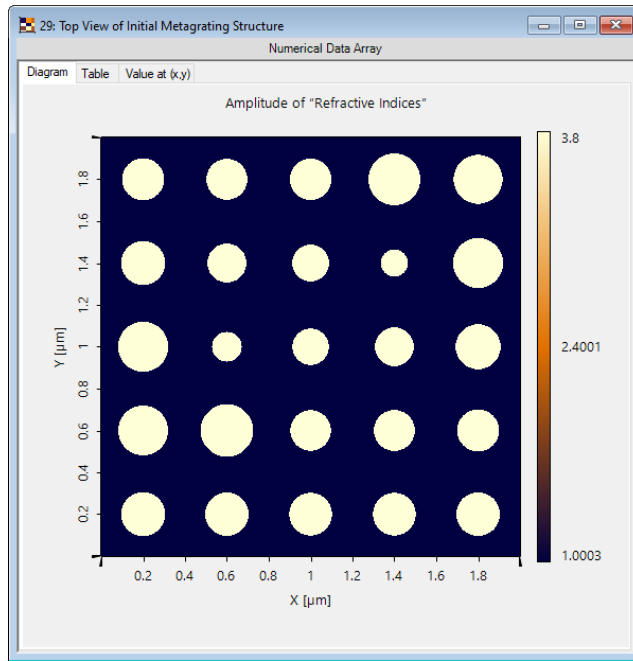


Overall efficiency	79.4%
Uniformity error (PV)	22.7%
Uniformity error (RMS)	16.7%

2D Metagrating_03_Initial Metagrating

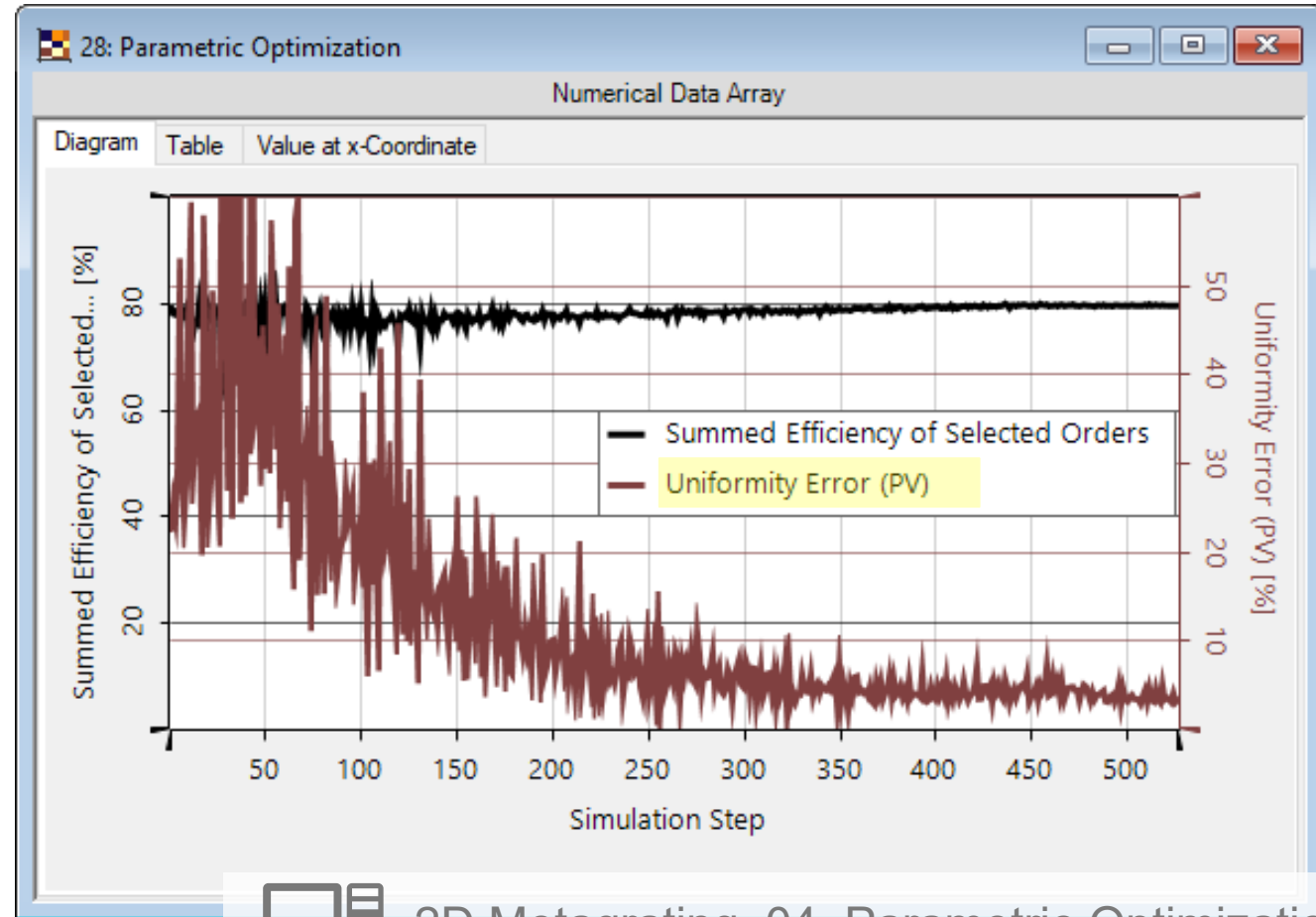
Post-Optimization of Metagrating (PV Uniformity Error)

initial structure



- keep pillar positions
- varying pillar diameters
- 25 variables in total

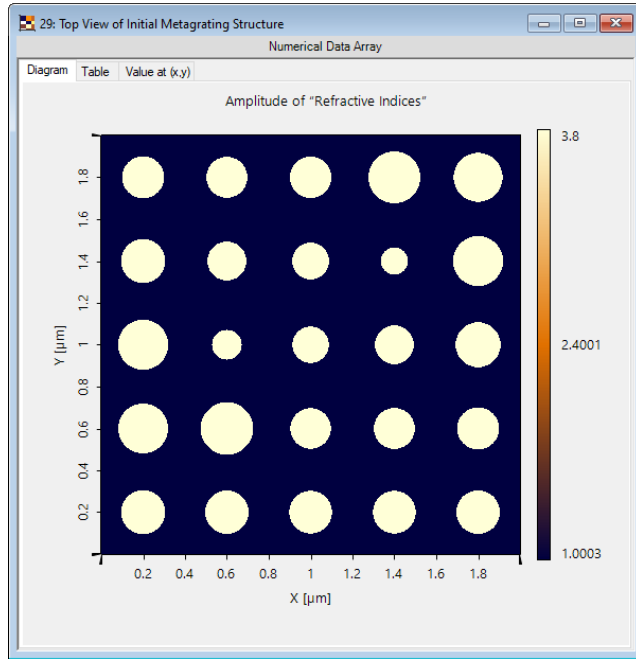
downhill simplex optimization with FMM/RCWA for grating analysis



2D Metagrating_04_Parametric Optimization

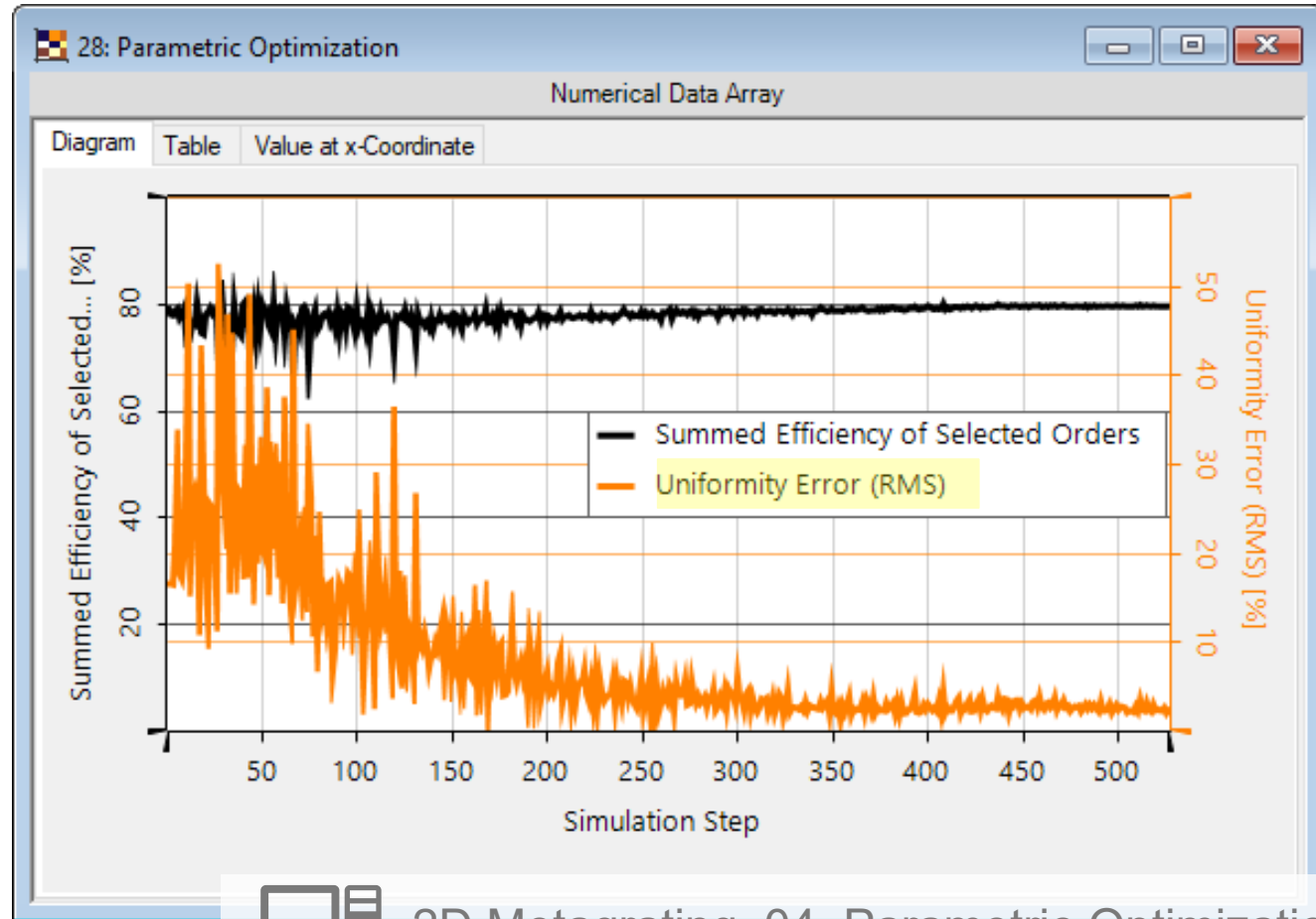
Post-Optimization of Metagrating (RMS Uniformity Error)

initial structure



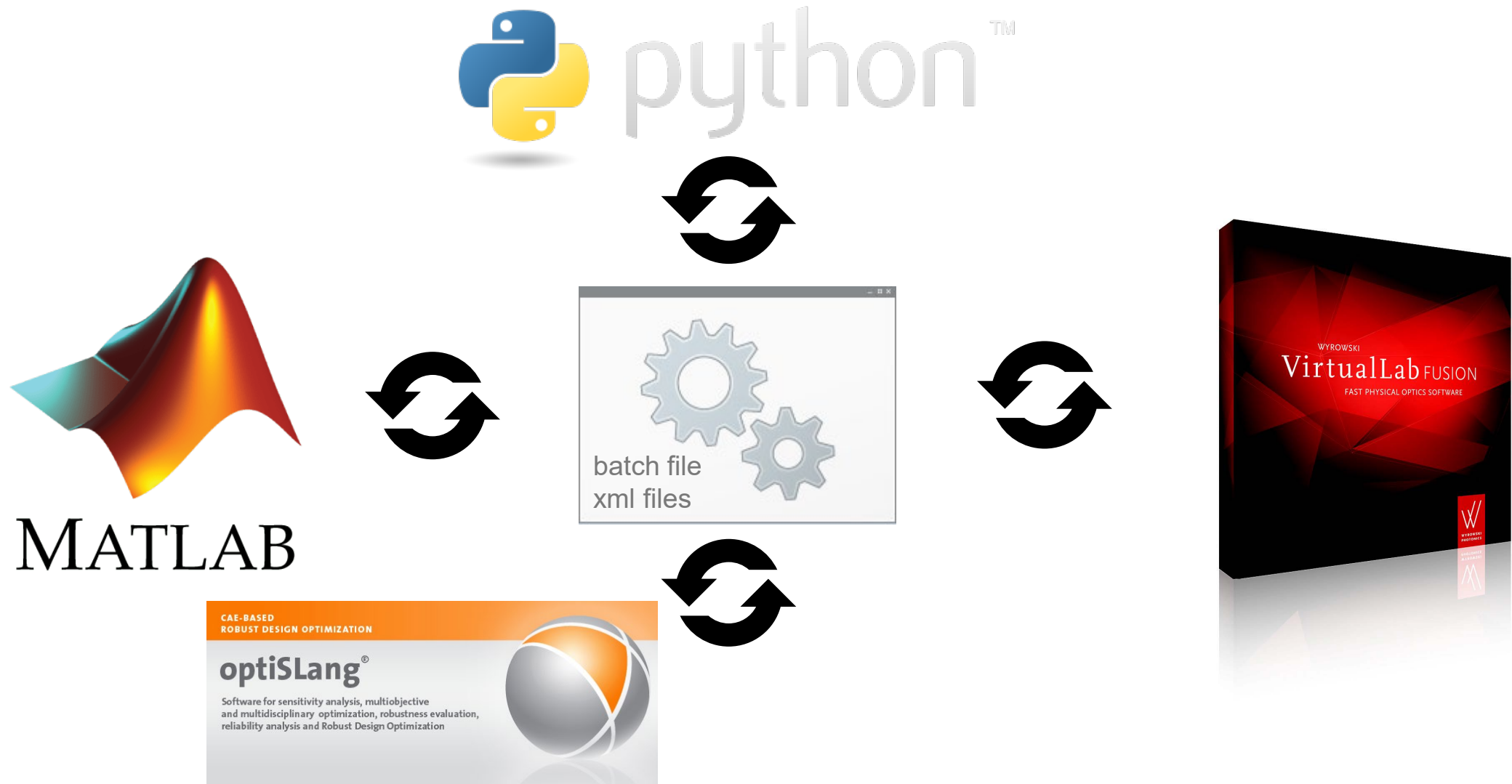
- keep pillar positions
- varying pillar diameters
- 25 variables in total

downhill simplex optimization with FMM/RCWA for grating analysis



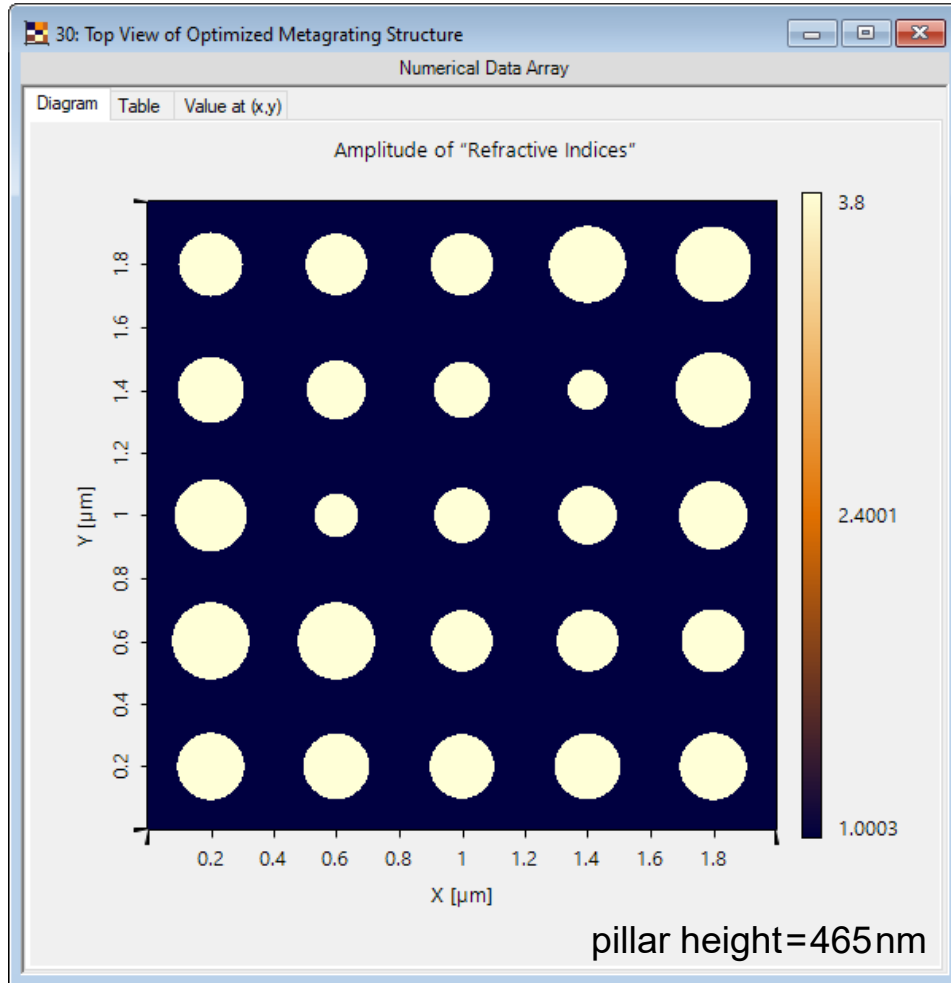
2D Metagrating_04_Parametric Optimization

Cross-Platform Simulation and Optimization

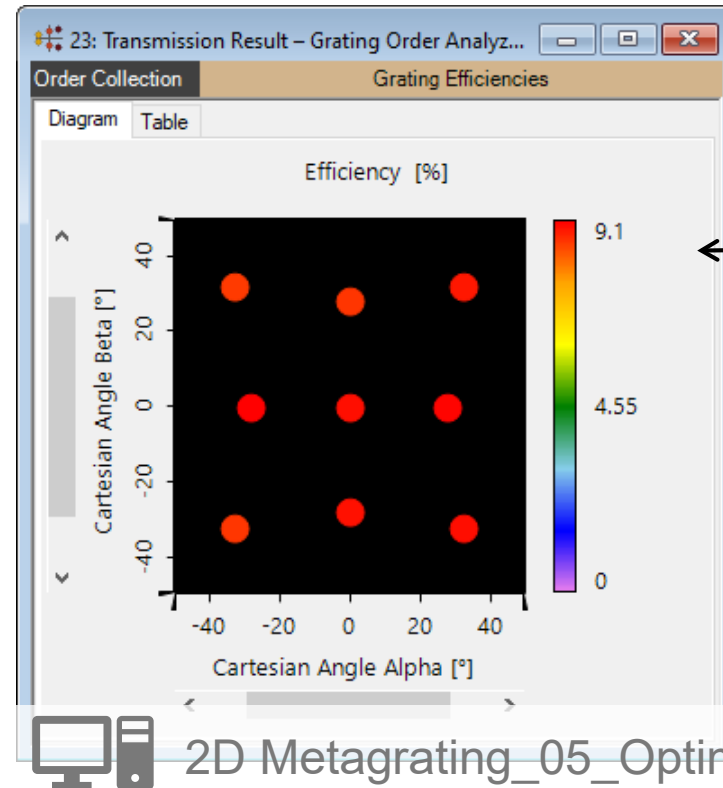


Evaluation of Optimized Metasurface Design

top view of optimized metagrating



diffraction efficiencies

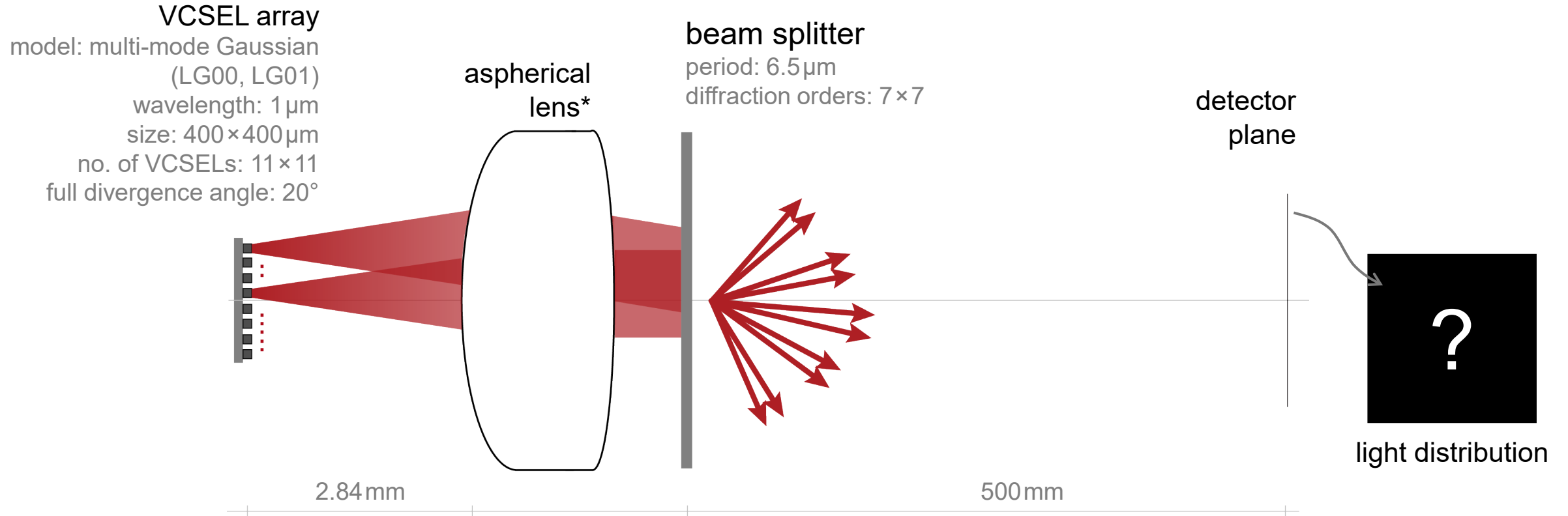


Overall efficiency	79.7%
Uniformity error (PV)	3.1%
Uniformity error (RMS)	2.3%

2D Metagrating_05_Optimized Metagrating

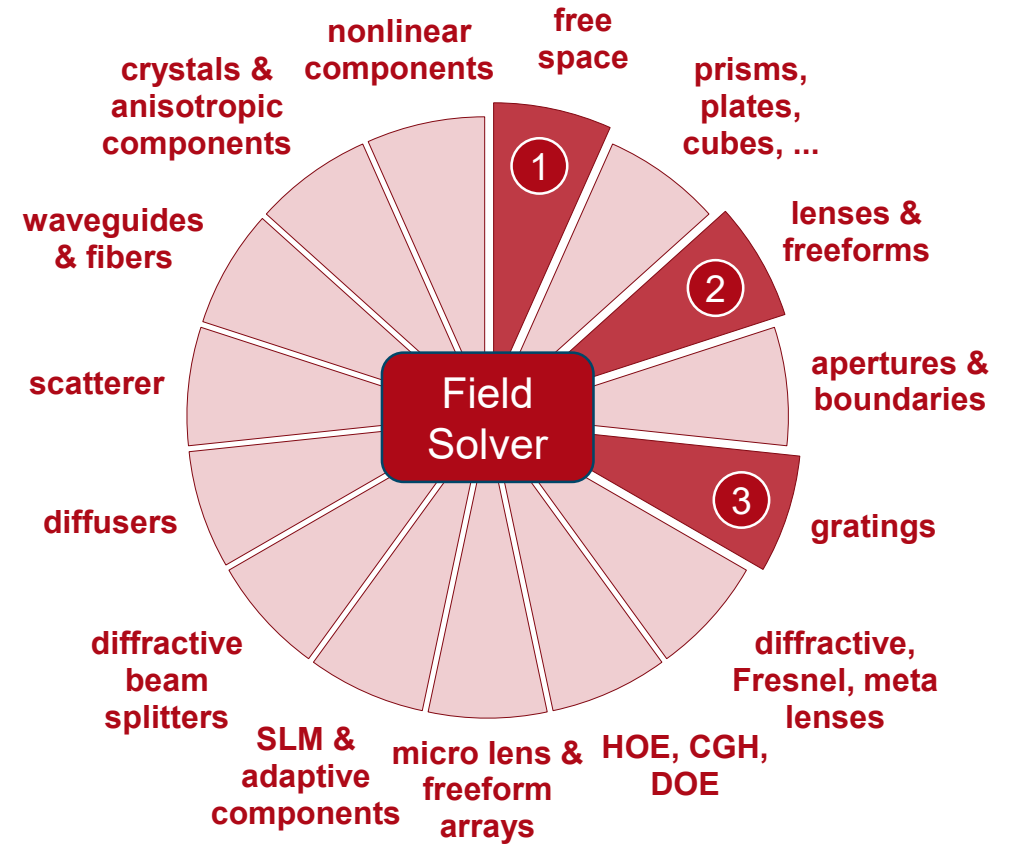
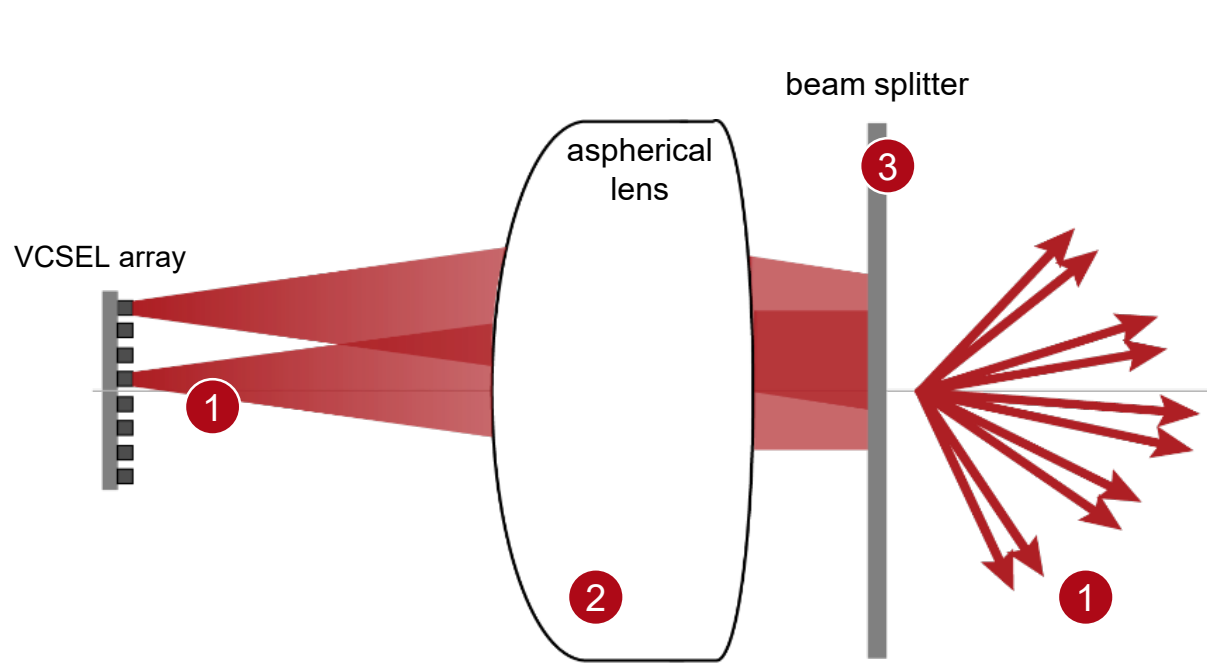
Modeling a VCSEL-Based Spot Projector

Modeling Task

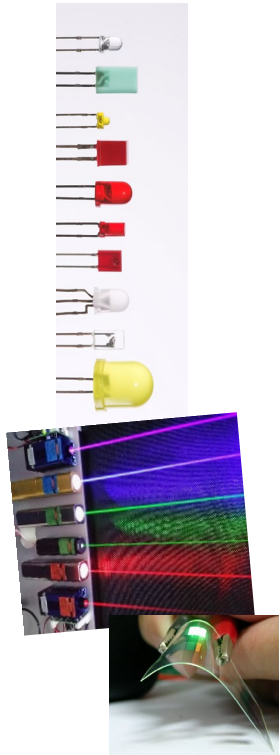


* The aspherical lens in the document is designed with Zemax OpticStudio®

VirtualLab Fusion Technologies



Source Modeling: Mode Decomposition for VCSEL



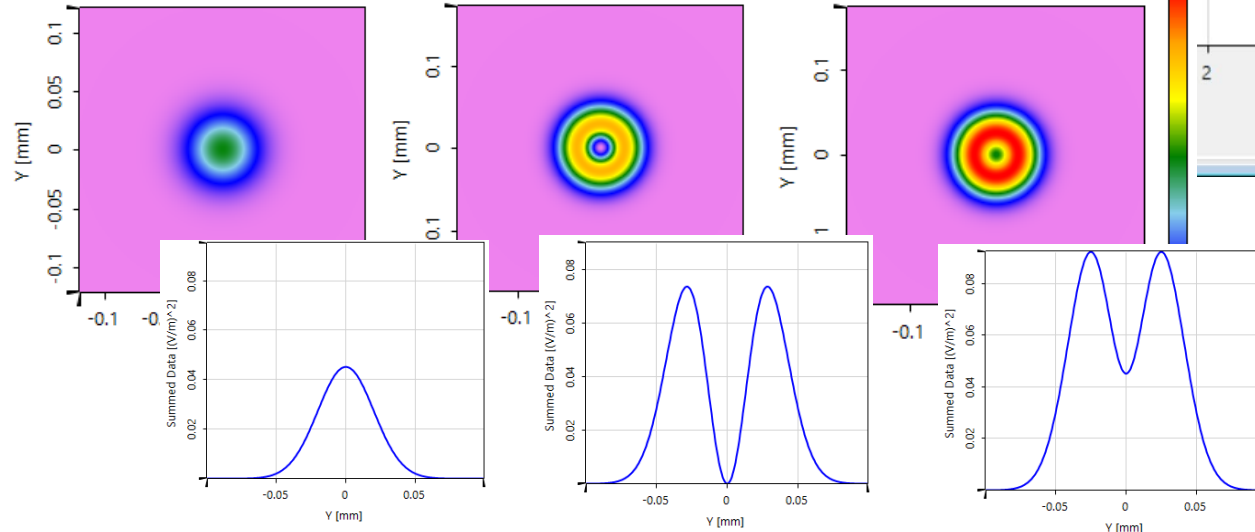
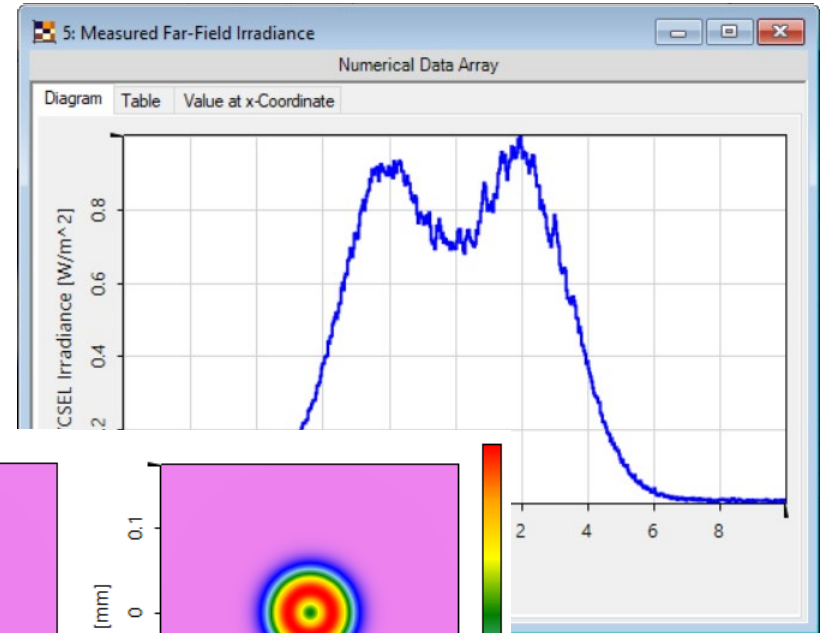
Source



Source modes

- Laser
- Laser diode
- LED
- OLED
- Lamp
- Natural light

fitting according to real-world measurement?



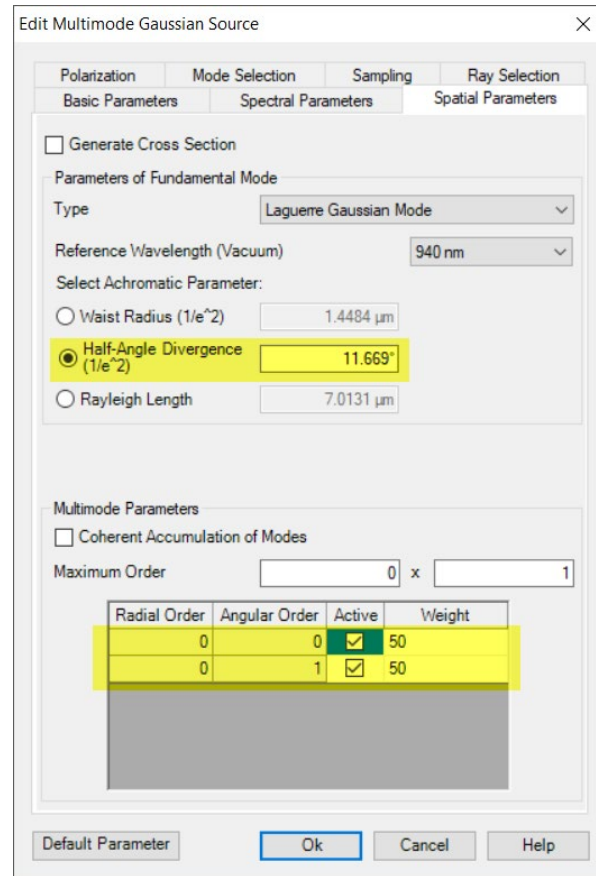
Mode (0, 0)

Mode (0, 1)

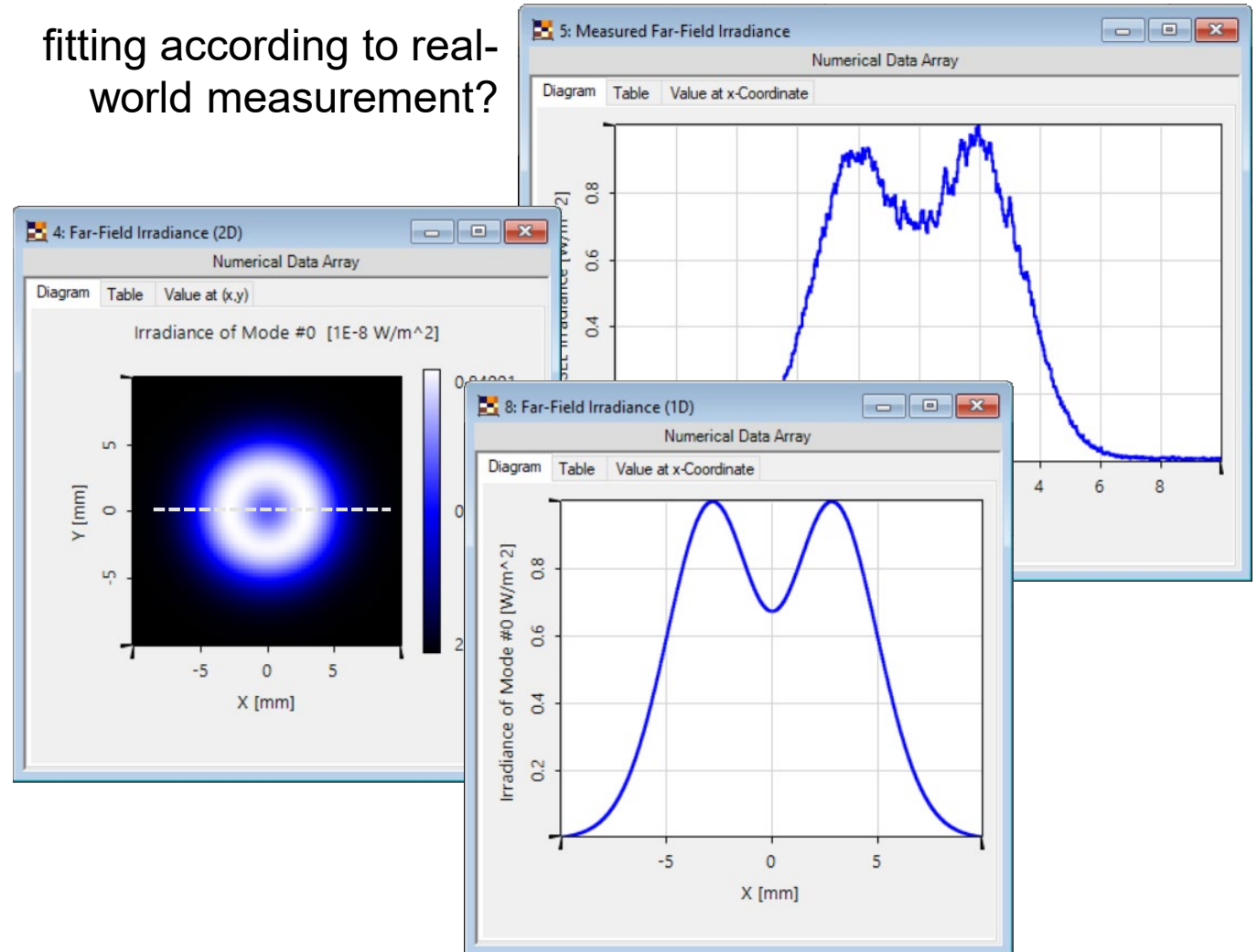
Sum

Source Modeling: Mode Decomposition for VCSEL

Initial test source

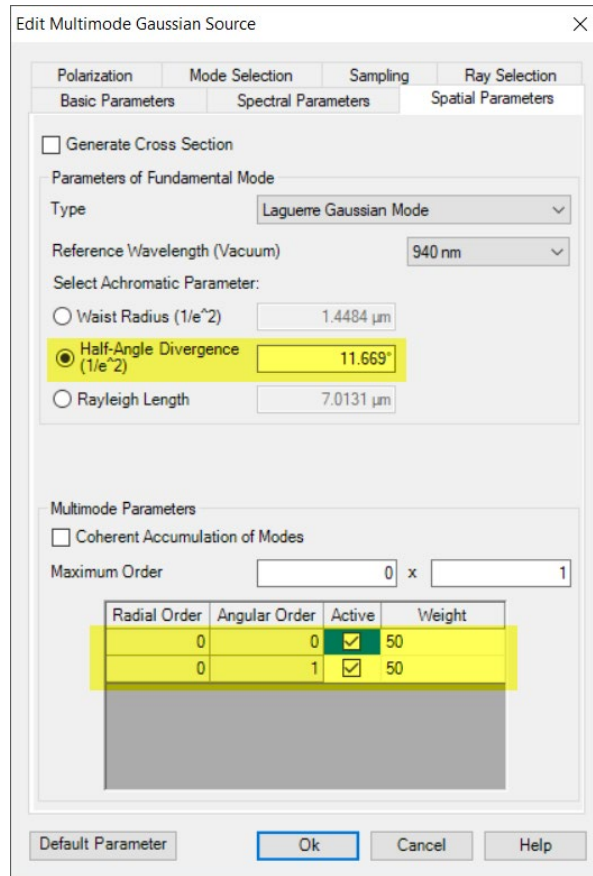


fitting according to real-world measurement?

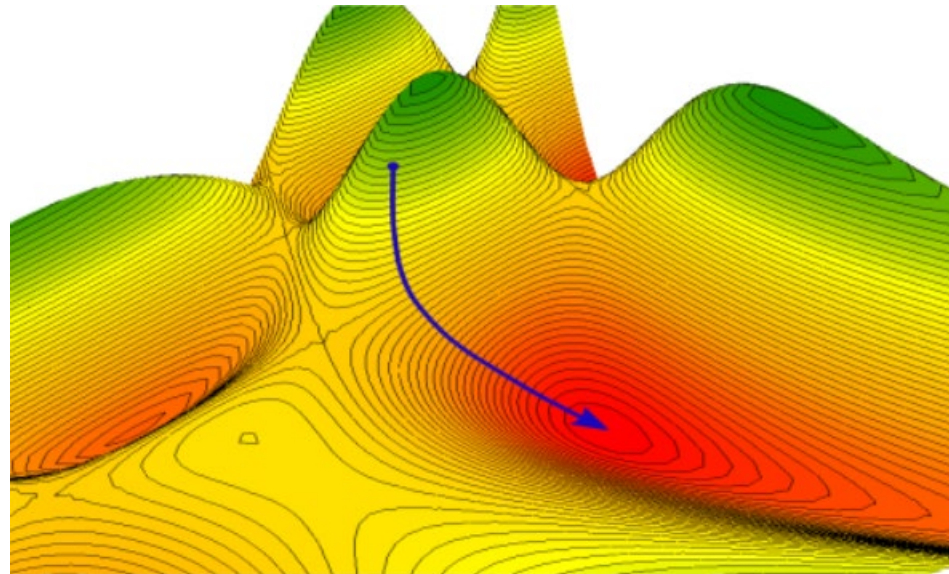


Source Modeling: Mode Decomposition for VCSEL

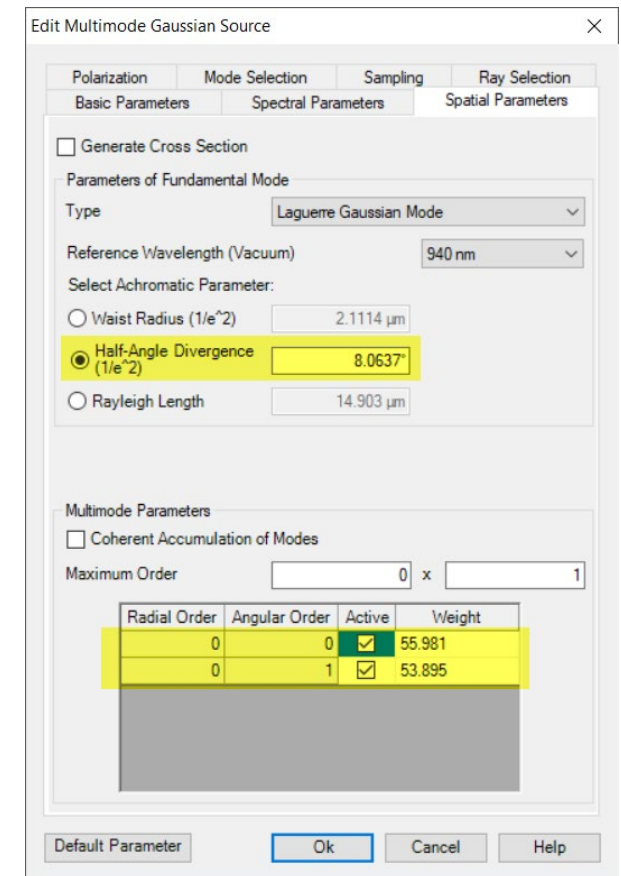
Initial test source



parametric optimization
(downhill simplex)

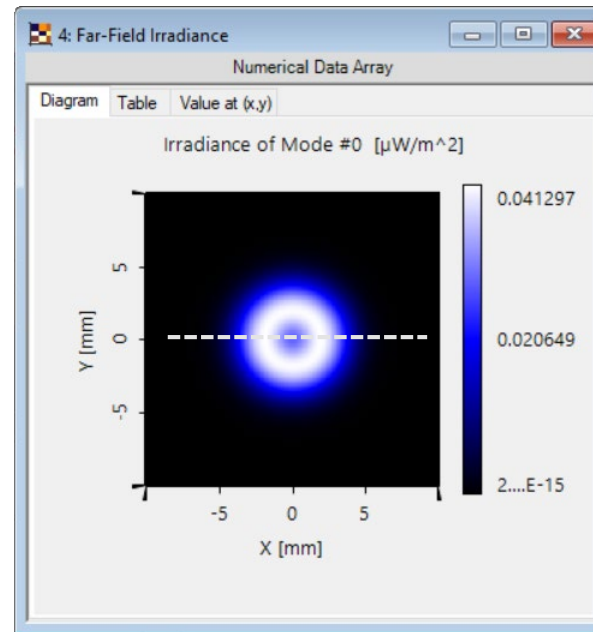
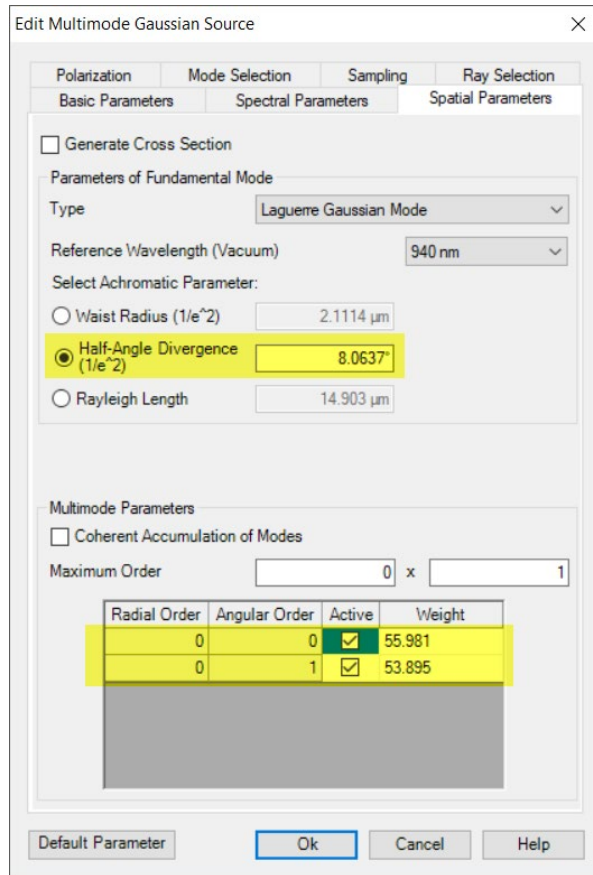


After parametric optimization



Source Modeling: Mode Decomposition for VCSEL

After parametric optimization



Source Modeling: Mode Decomposition for VCSEL

After parametric optimization

Edit Multimode Gaussian Source

Polarization Mode Selection Sampling Ray Selection
Basic Parameters Spectral Parameters Spatial Parameters

Generate Cross Section

Parameters of Fundamental Mode

Type: Laguerre Gaussian Mode

Reference Wavelength (Vacuum): 940 nm

Select Achromatic Parameter:

Waist Radius ($1/e^2$): 2.1114 μm

Half-Angle Divergence ($1/e^2$): 8.0637°

Rayleigh Length: 14.903 μm

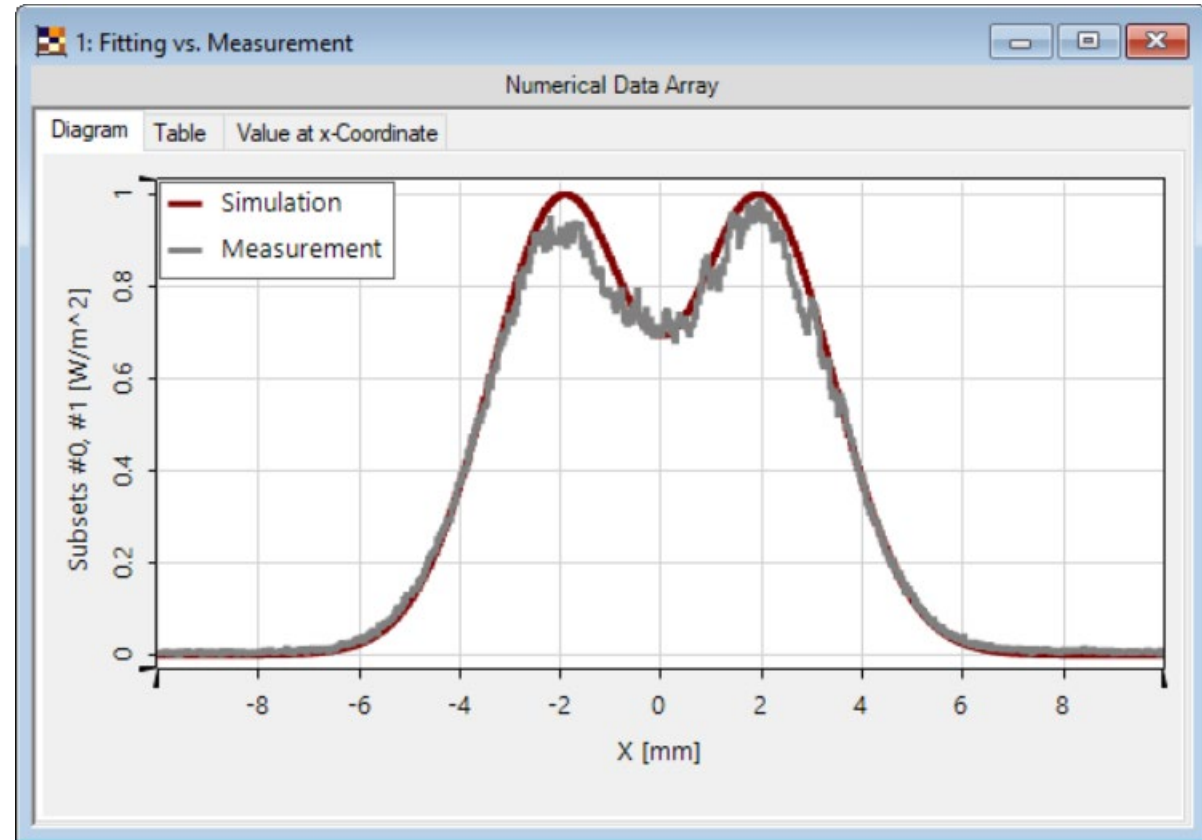
Multimode Parameters

Coherent Accumulation of Modes

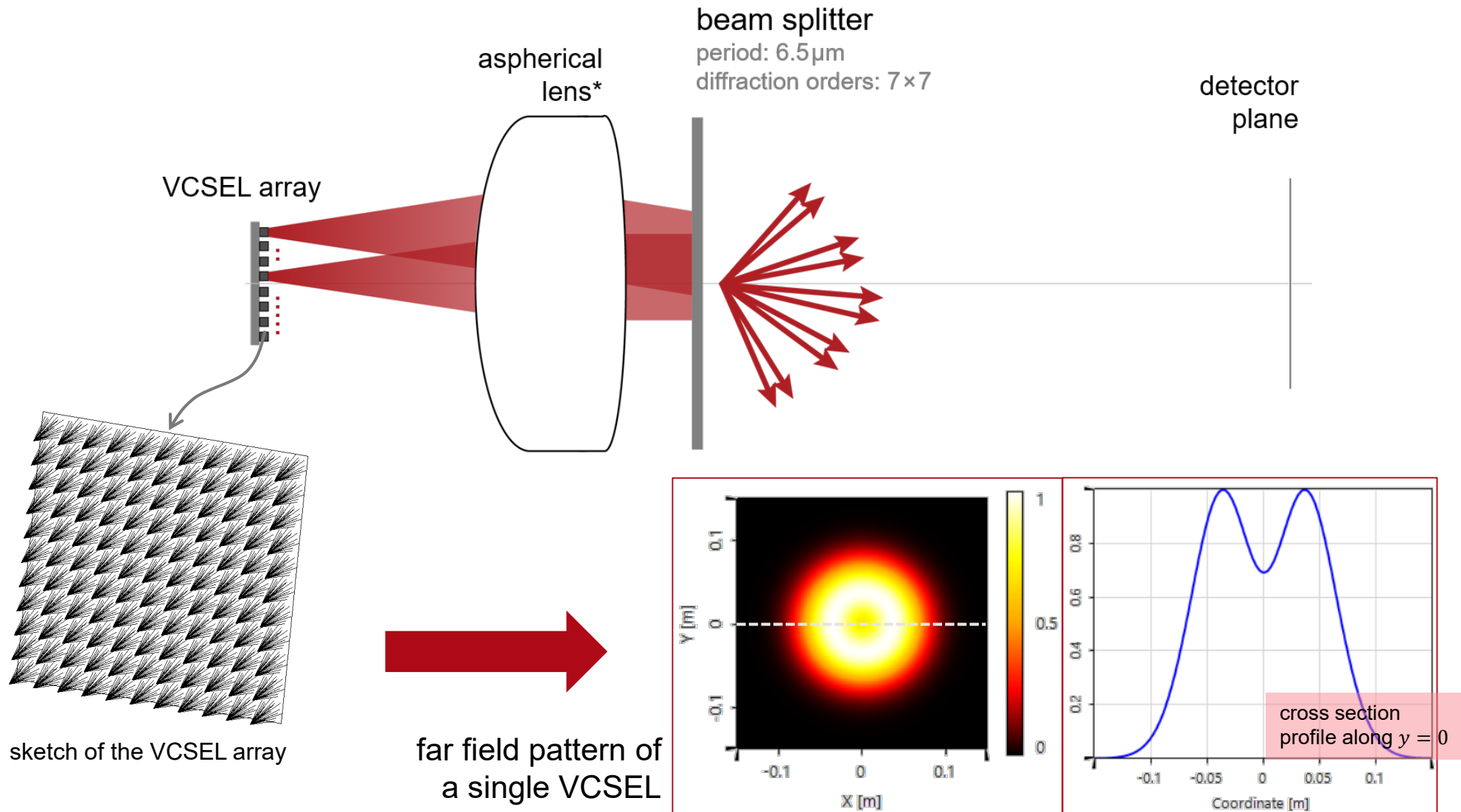
Maximum Order: 0 x 1

Radial Order	Angular Order	Active	Weight
0	0	<input checked="" type="checkbox"/>	55.981
0	1	<input checked="" type="checkbox"/>	53.895

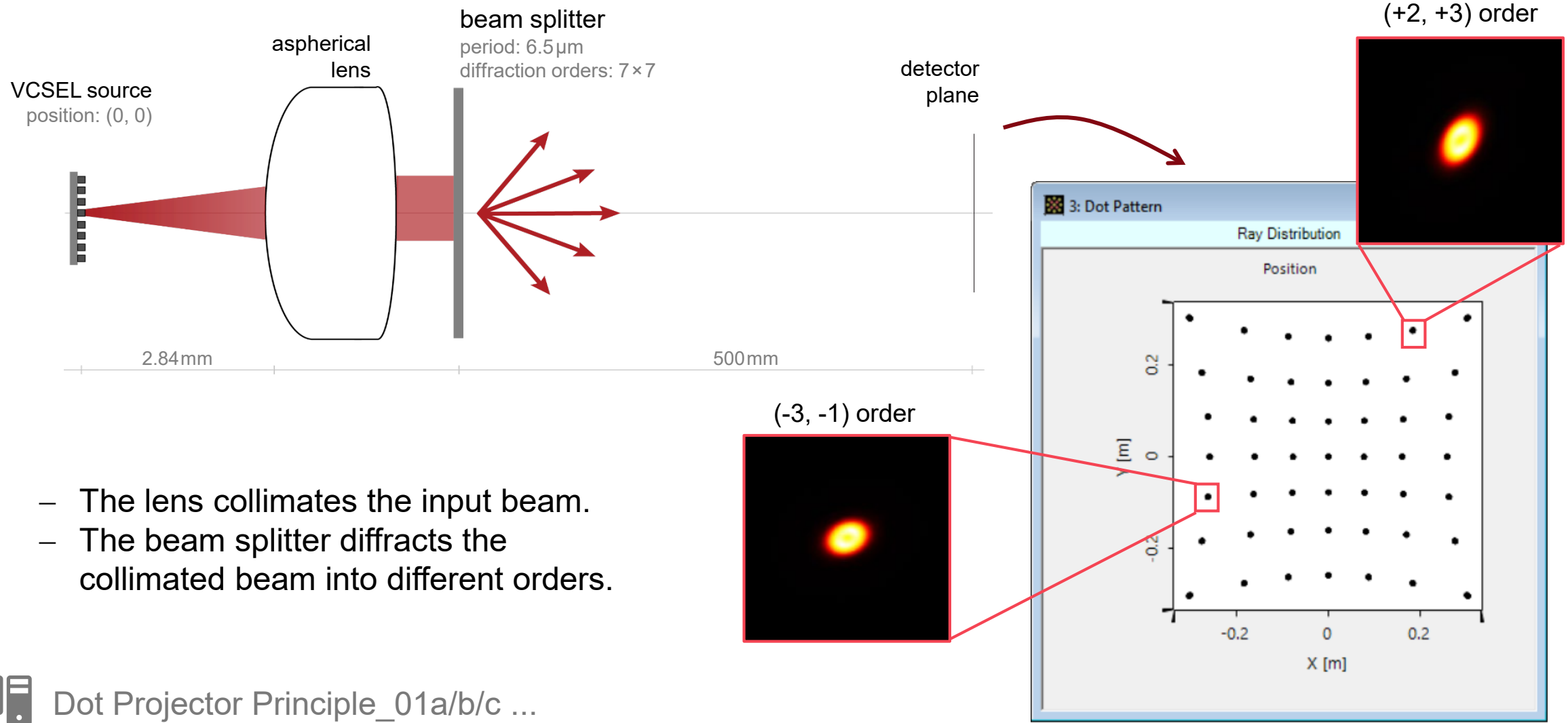
Default Parameter Ok Cancel Help



Source Modeling

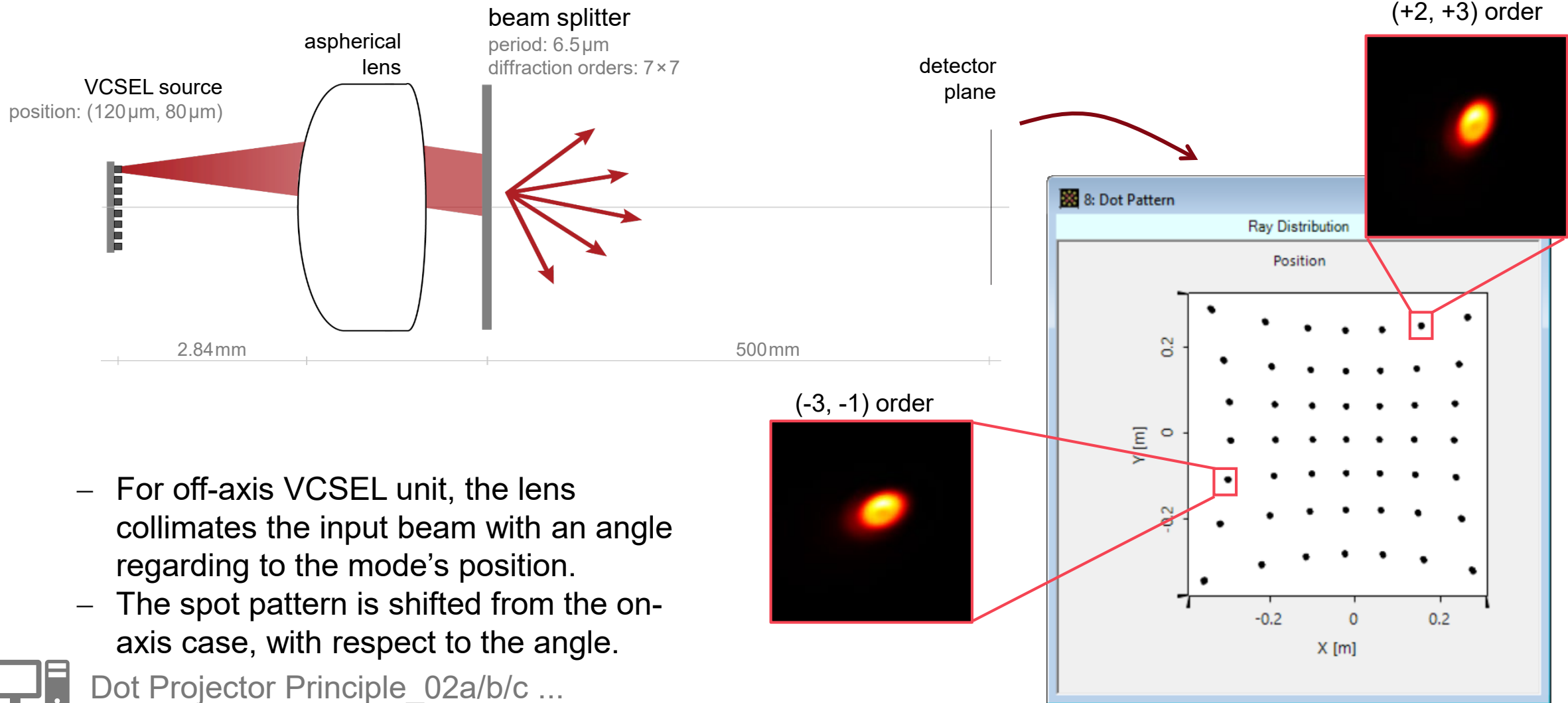


Simulation with the On-Axis VCSEL Unit



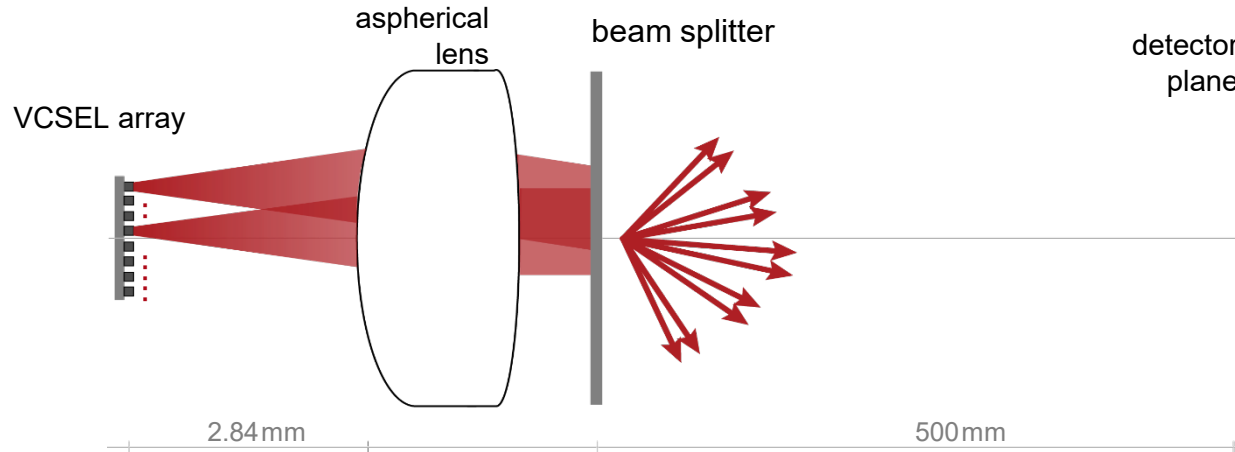
- The lens collimates the input beam.
- The beam splitter diffracts the collimated beam into different orders.

Simulation with an Off-axis VCSEL Unit



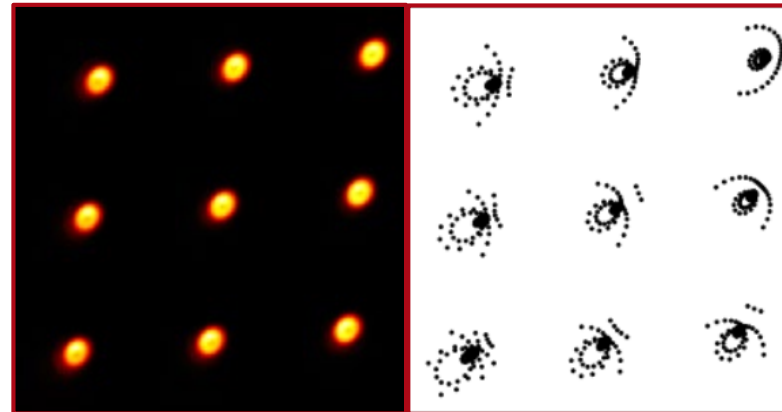
Dot Projector Principle_02a/b/c ...

Simulation with Complete VCSEL Array



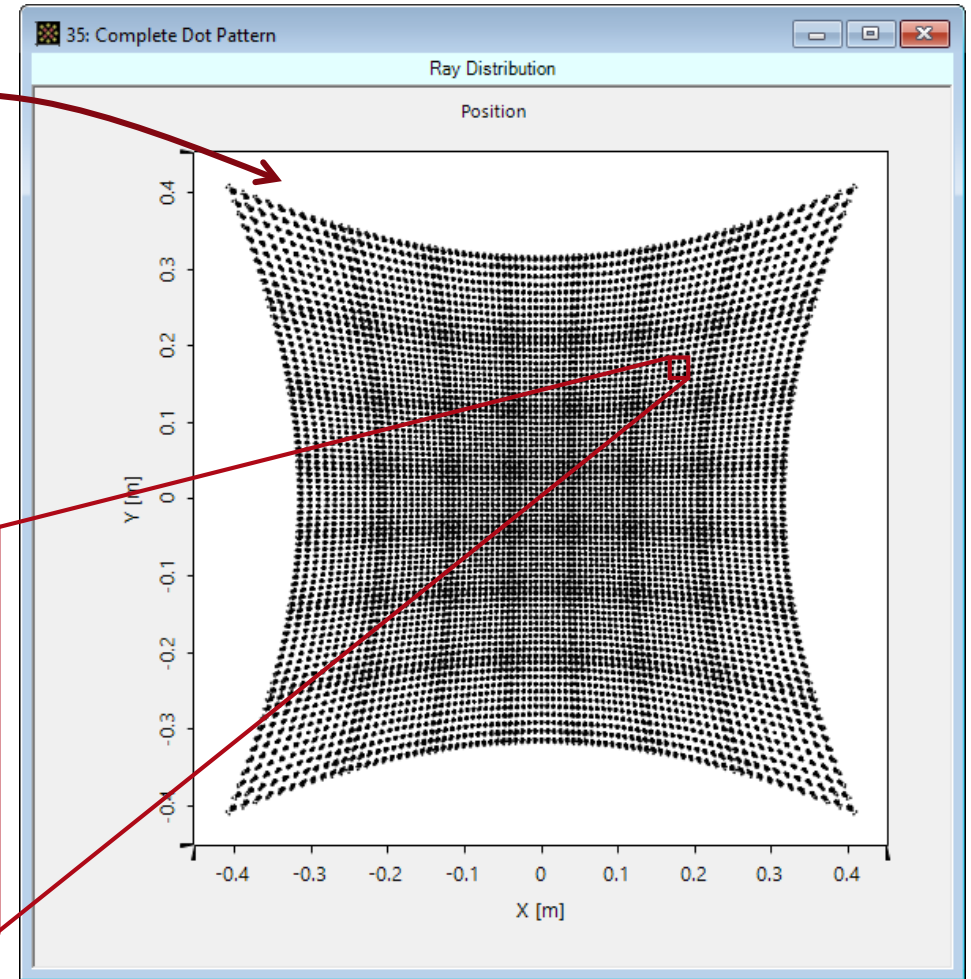
simulation results

The beam splitter duplicates the pattern of the VCSEL array with lateral shifts on the detector plane.

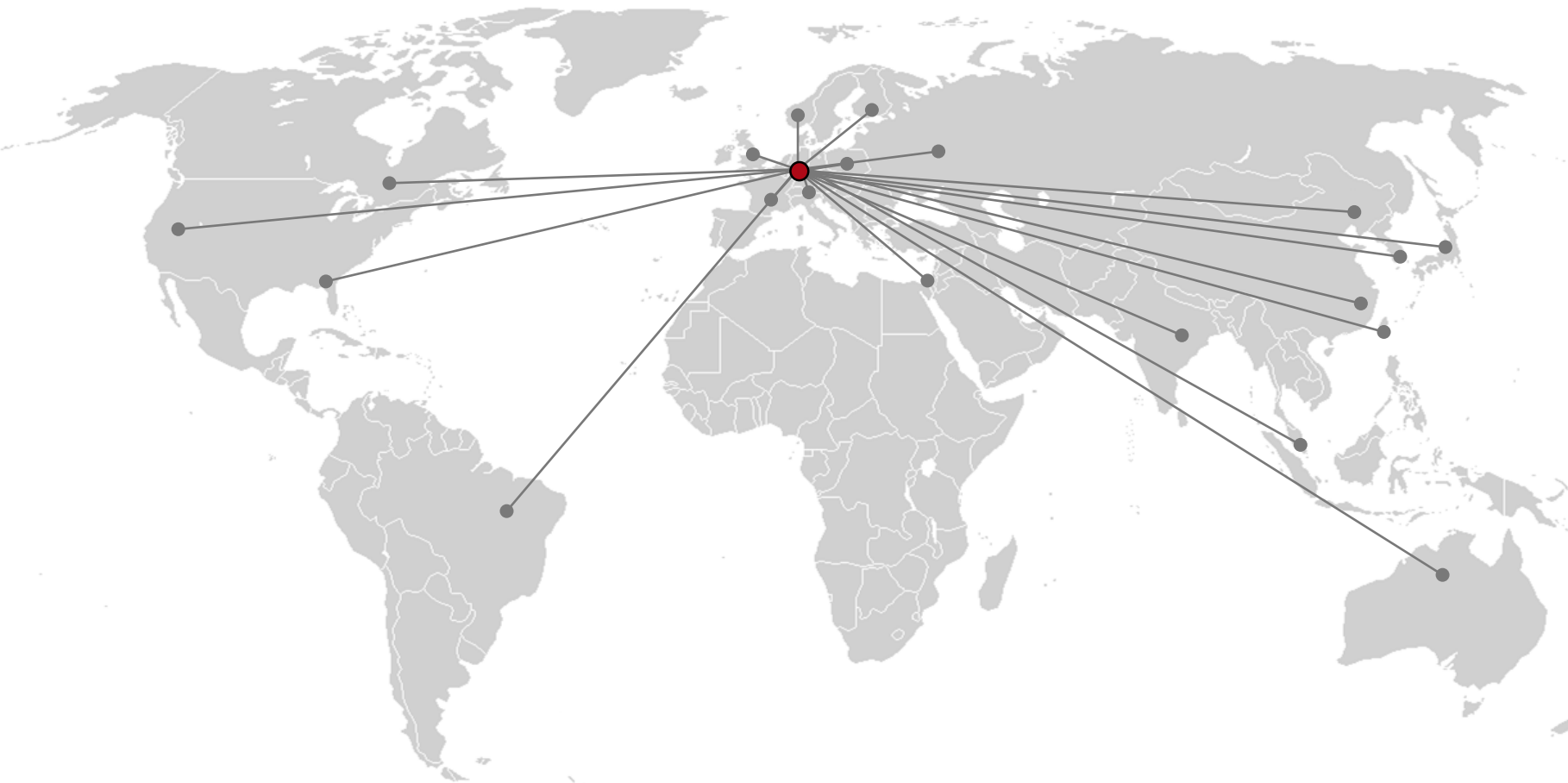


field tracing

ray tracing



Optical Design Software and Services



**Booth #4545
(German pavilion)**

